A neural network for tics: insights from causal brain lesions and deep brain stimulation

Christos Ganos[1,†], Bassam Al-Fatly[1,†], Jan-Frederik Fischer[1], Juan-Carlos Baldermann[2,3], Christina Hennen[2], Veerle Visser-Vandewalle[4], Clemens Neudorfer[1], Davide Martino[5,6], Jing Li[7], Tim Bouwens[8], Linda Ackermanns[8], Albert F. G. Leentjens[9], Nadya Pyatigorskaya[10], Yulia Worbe[11], Michael D Fox[7,12], Andrea A Kühn[1,†] and Andreas Horn[1,†]

[†]**These authors contributed equally to this work.**

Abstract

Brain lesions are a rare cause of tic disorders. However, they can provide unique insights into tic pathophysiology and can also inform on possible neuromodulatory therapeutic targets. Based on a systematic literature review, we identified 22 cases of tics causally attributed to brain lesions and employed 'lesion network mapping' to interrogate whether tic-inducing lesions would be associated with a common network in the average human brain. We probed this using a normative functional connectome acquired in 1,000 healthy participants. We then examined the specificity of the identified network by contrasting tic-lesion connectivity maps to those seeding from 717 lesions associated with a wide array of neurological and/or psychiatric symptoms within the Harvard Lesion Repository. Finally, we determined the predictive utility of the tic-inducing lesion network as a therapeutic target for neuromodulation. Specifically, we collected retrospective data of 30 individuals with Tourette disorder, who underwent either thalamic (n = 15; centromedian/ventrooralis internus) or pallidal (n = 15; anterior segment of globus pallidus internus) deep brain stimulation and calculated whether connectivity between deep brain stimulation sites and the lesion network map could predict clinical improvements. Despite spatial heterogeneity, tic-inducing lesions mapped to a common network map, which comprised the insular cortices, cingulate gyrus, striatum, globus pallidus internus, thalami, and the cerebellum. Connectivity to a region within the anterior striatum

(putamen) was specific to tic-inducing lesions when compared with control lesions. Connectivity between deep brain stimulation electrodes and the lesion network map was predictive of tic improvement, regardless of the deep brain stimulation target. Taken together, our results reveal a common brain network involved in tic generation which shows potential as a therapeutic target for neuromodulation.

Author affiliations:

[1]Charité – Universitätsmedizin Berlin, corporate member of Freie Universität Berlin and Humboldt-Universität zu Berlin, Movement Disorders and Neuromodulation Unit, Department of Neurology with Experimental Neurology, 10117, Berlin, Germany
[2]Department of Psychiatry and Psychotherapy, Faculty of Medicine and University Hospital Cologne, University of Cologne, 50931, Cologne, Germany.
[3]Department of Neurology, Faculty of Medicine and University Hospital Cologne, University of Cologne, 50931, Cologne, Germany
[4]Department of Stereotactic and Functional Neurosurgery, Faculty of Medicine and University Hospital Cologne, University of Cologne, 50931, Cologne, Germany
[5]Department of Clinical Neurosciences, University of Calgary, Calgary, 3330, Alberta, Canada.
[6]Hotchkiss Brain Institute, Calgary, 3330, Alberta, Canada.
[7]Center for Brain Circuit Therapeutics, Department of Neurology, Psychiatry, and Radiology, Brigham and Women's Hospital, Harvard Medical School, Boston, MA 02115, USA.
[8]Department of Neurosurgery, Maastricht University Medical Centre, 6229 HX, Maastricht, Netherlands.
[9]Department of Psychiatry, Maastricht University Medical Centre, 6229 HX, Maastricht, Netherlands
[10]Sorbonne University, Paris Brain Institute - ICM, Inserm, CNRS, Department of Radiology, Hôpital de la Pitié Salpêtrière (DMU 6), AP-HP, 75013 Paris, France.
[11]Sorbonne University, ICM, Inserm, CNRS, Department of Neurophysiology, Hôpital Saint Antoine (DMU 6), AP-HP, 75013, Paris, France.
[12]Athinoula A. Martinos Centre for Biomedical Imaging, Department of Neurology and Radiology, Massachusetts General Hospital, Charlestown, MA 02129, USA.

Correspondence to: Andreas Horn
Movement Disorders and Neuromodulation Unit
Department of Neurology
Charité University Medicine Berlin
Charitéplatz 1, 10117 Berlin, Germany
E-mail: andreas.horn@charite.de

Running title: Lesion and DBS network mapping of tics

Key words: brain lesions; tic disorders; lesion network mapping; deep brain stimulation.

Abbreviations: ANTs = Advanced Normalization Tools; BOLD = Blood-Oxygen-Level-Dependent; DBS = Deep Brain Stimulation; CM-Voi = Centromedian and Ventrooralis internus nuclei of the thalamus; FSL = Functional Magnetic Resonance Imaging of the Brain Software Library; FWE = Family-wise error; GPi = Globus Pallidus internus; LNM = Lesion Network Map; MNI = Montreal Neurological Institute; PaCER = Precise and Convenient Electrode Reconstruction for Deep Brain Stimulation; PALM = Permutation Analysis of Linear Models; Pf = parafascicular nucleus of thalamus.

Introduction

Tics are brief and sudden movements or sounds that resemble voluntary actions, but occur repetitively and without embedment to discernible context [1]. Tics may have multiple etiologies, but they are most encountered as part of a neurodevelopmental disorder spectrum, including Tourette disorder, which affects about 1% of children. There has been a long-standing debate about the pathophysiological underpinnings of tics and in the past few decades there have been numerous efforts to identify the neuronal locus – or network – that leads to their emergence[2,3].

The basal ganglia have been suggested as key neuronal structures in tic genesis [4]. This was driven by neuropathological studies, which identified abnormalities within motor and

associative functional domains of the striatum and globus pallidus internus (GPi)[5,6], and therapeutic interventions, such as deep brain stimulation (DBS) that targeted these areas. Building on ablational studies by Hassler and Diekmann[7], a first report on a patient treated with DBS targeting the border between centromedian and ventrooralis internus nuclei of the thalamus (CM-Voi) was published in 1999[8]. Since then, DBS targeting i) this target [9,10], ii) the anterior vs. posterior ventrooralis nuclei in Hassler nomenclature[11] (or ventroanterior/ventrolateral thalamus according to Jones Nomenclature [12]) iii) the anteromedial [13,14] and iv) the posteroventral [15] GPi has been demonstrated to effectively reduce tics. More recently low-frequency tic-related neuronal activity was recorded in GPi and CM-Voi in Tourette patients undergoing DBS suggesting an electrophysiological correlate in tic pathophysiology[16-18].

Outside the basal ganglia, cortical neurophysiology studies have implicated the supplementary motor area and primary motor cortex in tic occurrence [17,19-22]. Structural and functional neuroimaging studies further revealed an extensive network of additional brain areas involved in the generation of tics (reviewed by Martino et al. [23]), including the prefrontal and cingulate cortices [24-26], the primary somatosensory area [24,25,27-30], the parietal operculum [31,32], and the insula [27,31-33].

These and other studies suggest that tics are not the result of a single dysfunctional brain region, but rather emerge in consequence of critical alterations at different cortical and subcortical hubs within a widespread neural circuit [24,34]. However, a causal role of different brain regions for tic generation remains elusive. Moreover, while some regions described in functional (correlative) studies may contribute to tic expression, others could indeed be involved in symptom compensation.

Studies of brain lesions and brain stimulation results are among the few general concepts that may justify causal inference [35]. More recently, it has become possible to map the impact of

specific lesions on distributed *brain networks*. The technique, termed *lesion network mapping* [36] uses normative functional connectomes acquired in large samples of healthy participants to investigate into which network a specific lesion would fall *in the average human brain*. So far, the method has provided insights into different neuropsychiatric symptoms [35], including movement disorders [37-39] and disorders of volition [40,41]. In a similar vein, a novel concept termed *DBS network mapping* has applied the same concept to stimulation sites [42]. Again, the method asks the question of which functional brain network a specific DBS stimulation site would fall *within the average human brain*. So far, the method has provided insights into effective neuromodulation networks in neurological disorders of movement [42-44] and psychiatric disorders [45,46]. Importantly, several papers have shown that both lesion and DBS network mapping provide convergent results, as for example in parkinsonism [38], dystonia [39] and depression [47].

The aim of this study was to shed light onto the networks associated with tic generation using combined brain lesion and DBS network mapping. To this end, we carried out a systematic review of the medical literature to collect brain lesions that were involved in the occurrence of tics and determined the common functional network underlying most lesions. To assess the therapeutic relevance of this network, we predicted clinical outcomes in patients with Tourette disorder who received therapeutic deep brain stimulation (either in the CM-Voi of thalamus or GPi) from three different DBS centres (Cologne, Paris and Maastricht).

Materials and methods

Cases and lesion definition

Methods of the review were developed by two members of the author team (CG, JF) prior to conducting the review. In March 2020 PubMed (MEDLINE 1966-2020) and EMBASE (1947-

2020) were searched with a combination of free-text, MeSH Terms, and truncated words (see supplementary material). To be included, papers needed to meet pre-defined inclusion criteria: a) English reports describing b) patients (case reports, case series, letters, and observational studies), with c) new-onset tics attributed to d) lesions of the CNS, e) lesion location shown by neuroimaging that was further described in writing. After removal of duplicates results were screened by title and abstract. The first 50 abstracts were screened by two reviewers (JFF, CG) to control for interpersonal agreement and subsequent results were screened by one author (JFF). Eligible, and available records were then read in full text subsequently. If the single reviewer had questions about the potential full-text inclusion of an article, the full text was then reviewed with the first author (CG) for discussion. Risk of bias assessment was not applicable. Details on the number of results and the process of literature search are listed in Supplementary Fig. 1. We did not apply a temporal restriction criterion between the clinical manifestation of tics and the documentation of brain lesions to capture as many different etiologies as possible. In cases where the manifestation of tics was the only clinical event associated with a brain lesion, we captured the latency between the two. In all other cases, where an additional clinical syndrome preceded the onset of tics and was attributed to documented brain damage, we captured the time lag between this event, tic behaviors and lesion confirmation. We excluded reports about "tic-like" phenomena, which may subsume functional tic disorders or overlap syndromes, as well as drug-induced tics and cases of tics associated with traumatic events of the peripheral nervous system. Reports of tic improvement associated with brain lesions (e.g., through neurosurgery) were not considered. Cases with characteristic brain malformations associated with known, mostly neurodevelopmental, genetic syndromes and tic disorders were also excluded. Review articles were included for cross-referencing in the first step.

From the included reports we extracted the following data: 1) study characteristics (study type, year of publication); 2) patient characteristics (age of assessment, sex, medical history, type of clinical event and age at time of occurrence); 3) clinical characteristics of tics (predisposing

factors, pre-existing tics and their characteristics, latency between first confirmation of lesions and tic onset/worsening, motor/vocal forms, tic somatotopy, suppressibility/ premonitory urges, waxing and waning course, neuropsychiatric comorbidities, therapeutic strategy and outcome and additional video documentation); 4) characteristics of documented brain lesion (attributed etiology, anatomical localization and modality of neuroimaging, age at confirmation of lesion). Lesion locations were identified from corresponding publication figures and manually traced using 3D Slicer (www.slicer.org) on a common T1 template available within ICBM2009b NLIN Asym ("MNI") space.

Lesion network mapping

Each binary lesion mask was entered as a seed using the Lead connectome mapper toolbox openly available within Lead-DBS (www.lead-dbs.org [48]). Seed-based connectivity was calculated using a normative fMRI connectome acquired at rest in 1,000 participants [49] that had been preprocessed as described elsewhere [50]. For each subject in the connectome, BOLD signal fluctuations across all voxels within the lesion mask were averaged and correlated to the BOLD signal of all other brain voxels using the Pearson correlation coefficient. This resulted in 1,000 *R*-values for each brain voxel (one per subject) which were Fisher-z-transformed. Using voxel-wise one-sample T-tests, these 1,000 *z*-values were summed up to an average connectivity profile map of T-scores. We will refer to this map as the T-map. Every lesion specific T-map was then thresholded to a T-score of 7 and binarized to represent the significant positive T-scores in each T-map. This threshold level was chosen based on previous experience in multiple lesion network mapping publications (see [51] for a discussion). Choosing a range of different thresholds largely did not alter the overall pattern of the result (Supplementary Fig. 2). In a next step, all lesion-specific binarized T-maps ($n = 22$) were summed up into a single N-map which represented a tic-inducing Lesion Network Map (LNM). The LNM was then thresholded to

include only voxels that received contribution from ≥ 19/22 lesions (86% of cases). This threshold was chosen upon visual inspection and the number of retained voxels, to define a set of regions most specifically connected to a maximum number of lesion cases (higher thresholds >20 or >21 retained little to no voxels, see Supplementary Fig. 3 for results with different thresholds).

Specificity of tic lesion network

We then aimed to explore whether specific sites within the tic-lesion network were not only sensitive but also specific to tics compared to other naturally occurring brain lesions. In order to do so, connectivity T-maps derived from tic-inducing lesions were compared to the ones from a total of 717 other brain lesions from the Harvard Lesion Repository [35]. This repository contains lesions associated with various neurological and/or psychiatric symptoms which are (numbers indicate lesion counts in each specific category): Akinetic Mutism, 28; Alien Limb, 53; Amnesia, 53; Aphasia, 12; Asterixis, 30; Cervical Dystonia, 25; Criminality, 17; Delusions, 32; Depression, 58; Freezing of gait, 14; Hemichorea 29, Hallucination: 89, Holmes' tremor, 36; Infantile Spasms, 74; Loss of consciousness, 16; Mania, 56; Pain, 22; Parkinsonism, 29; Prosopagnosia, 44. The specificity map was calculated using a voxel-wise permutation-based 2-sample T-test performed (with 1000 permutations) within FSL PALM (https://fsl.fmrib.ox.ac.uk/fsl/fslwiki/Randomise/UserGuide). A rigorous voxel-wise FWE correction was then applied at $\alpha < 0.05$ to reduce false positive results [52] and highlight only the significant findings. Based on these results, we subsequently computed a 'conjunction map', on which voxels that were both specific and sensitive to tics were retained by multiplying the sensitivity (lesion network) map and the specificity map.

Relationship to DBS treatment

In a further step, we sought to investigate the relevance and potential clinical utility of the tic-inducing lesion network. We tested whether specific stimulation sites in a retrospective cohort of Tourette disorder patients treated with DBS that were maximally connected to the lesion network map would be associated with optimal outcomes. Pre- and postoperative imaging data from a total of 30 adult patients from three DBS centres with a diagnosis of Tourette disorder that underwent DBS surgery were used to localize DBS electrodes and specify stimulation sites in each patient.

Fifteen adult patients with Tourette disorder underwent DBS to thalamus nuclei (Cologne cohort; n = 12 in the centromedian-ventro-oralis and n = 3 in the nucleus ventroanterior/ventrolateral nucleus with the most distal contacts residing in the field of Forel/subthalamic nucleus) and 15 to the GPi (Paris and Maastricht cohorts). Localization of electrodes and estimation of stimulation volumes were carried out using Lead-DBS software (www.lead-dbs.org [48]). We applied default parameters of the revised pipeline [53]; briefly, this involved co-registration between postoperative MRI (n = 2) or CT (n = 28 patients) to preoperative anatomical MRIs using advanced normalization tools (ANTs; http://stnava.github.io/ANTs/[54]). The resulting co-registered images were then normalized to MNI space using the ANTs SyN Symmetric Diffeomorphic algorithm [54] using the "effective: low variance + subcortical refinement" preset in Lead-DBS. Electrodes were reconstructed using the PaCER [55] algorithm and manually refined, if necessary. Stimulation volumes were estimated using a finite element approach based on a four-compartment tetrahedral mesh (including white or grey matter, electrode insulating and conducting regions) [53]. The estimated E-field was thresholded to a heuristic value of 0.2 V/mm to calculate the extent of a binary volume. These were then used as seed regions – exactly analogous to brain lesions – to calculate

functional connectivity average T-scores representing average seed-based connectivity strength. T-scores were *z*-transformed to a Gaussian distribution following the approach of van Albada et al. [56] to serve as predictors of DBS associated tic-improvements.

In a last step, we sought to investigate how connectivity strength from stimulation sites of DBS cohorts to both sensitive and specific voxels of the maps, and their overlap (conjunction map) could explain tic-improvement. Similar to the analysis above, connectivity strength was again calculated between DBS stimulation sites and respective map. These coefficients were then correlated to tic-improvement.

DBS network mapping

In a final analysis, we aimed at characterizing the networks optimally modulated by each DBS site in a data-driven fashion. To do so, we applied DBS network mapping following the approach by Horn et al. [42] which follows a highly similar logic as the lesion network mapping approach. Briefly, DBS network maps were calculated in identical fashion to lesion network maps. We then correlated connectivity strength in each voxel with tic improvements, across patients, resulting in R-map models that approximate optimal connectivity profiles. Voxels with high values on these maps embody locations to which DBS electrodes that led to optimal improvement were strongly connected. We calculated these R-map models for each target cohort separately (pallidal and thalamic target). In a second step, we multiplied resulting maps with each other, but only retaining voxels that were positive on *both* maps. In doing so, we were able to pinpoint the network from two angles (pallidal and thalamic DBS sites). Therefore, this approach would likely clean the result from some spurious correlations and retain a higher fraction of regions that could indeed have causal implications [57].

Data availability

The DBS MRI/CT datasets generated and analysed during the current study are not publicly available due to data privacy regulations of patient data but are available from the corresponding author upon reasonable request. Lesion tracings and lesion network map are also available from corresponding author upon reasonable request. All code used to analyse the datasets is available within Lead-DBS /-Connectome software (https://github.com/leaddbs/leaddbs).

Results

The systematic review (see Supplementary Fig. 1 for flow-chart) identified 22 cases with new onset of tics attributed to brain lesions (see Supplementary Table 1). The mean age at tic onset was 25.3 years (± 20.7 SD, range 5-73 y; in two cases tic-onset age was not provided). In 12 cases, the latency between brain injury and tic onset could be reconstructed (see Supplementary Table 1). There were 2 cases with isolated motor and 2 with isolated vocal tics. The remaining 18 cases had both motor and vocal tics. Premonitory urges and tic suppressibility were documented in 10 and 12 cases, respectively. In 10 cases, additional movement disorders were also noted, including dystonia (n = 4), parkinsonism (n = 3), cerebellar ataxia (n = 2), tremor (n = 1) and stereotypies (n = 1). However, again, in these cases occurrence of tics was salient and novel following the brain lesion. Neuropsychiatric features, such as impulsivity and/or hyperactivity (n = 9), obsessive-compulsive (n = 5) and self-injurious behaviors (n = 3) were also reported.

Although the basal ganglia were the most commonly documented lesion site (n = 17), the locus of neuronal damage varied among cases, and often involved multiple brain areas (Fig. 1). Other brain areas included the temporal and parietal lobes, the insula, corpus callosum, thalamus,

internal capsule, midbrain, pons and medulla oblongata. Brain lesions occurred for different etiological reasons, ranging from traumatic brain injury to stroke, as well as infectious and inflammatory causes (Supplementary Table 1 provides the complete list of clinical and paraclinical case characteristics).

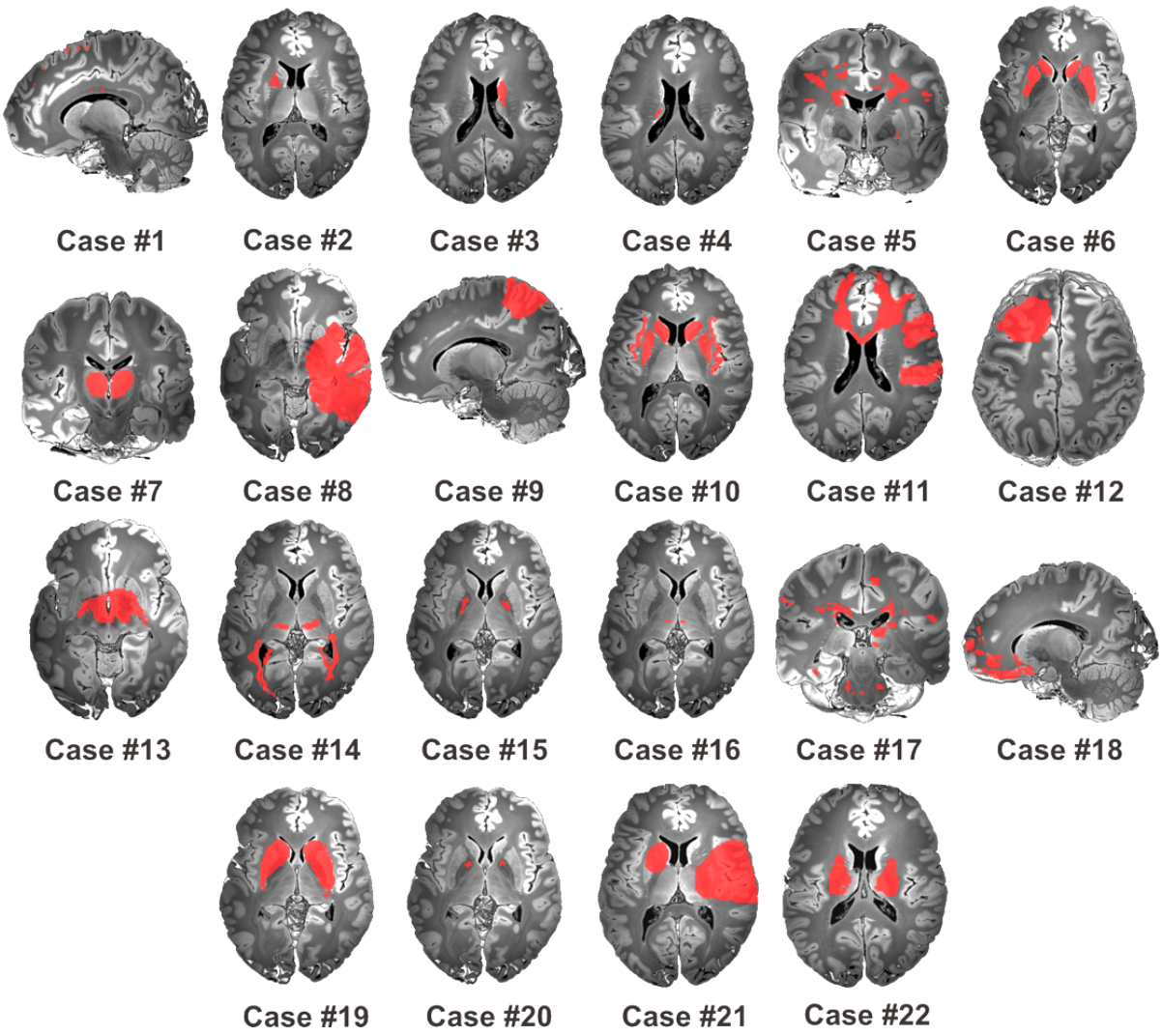

Figure 1 Tic-inducing lesions. The spatial distribution of lesion masks extracted from 22 case reports included in the current study mapped to a wide extent of brain regions. All binary masks were drawn in MNI space and visualized on an ultra-high resolution postmortem template for anatomical reference[58].

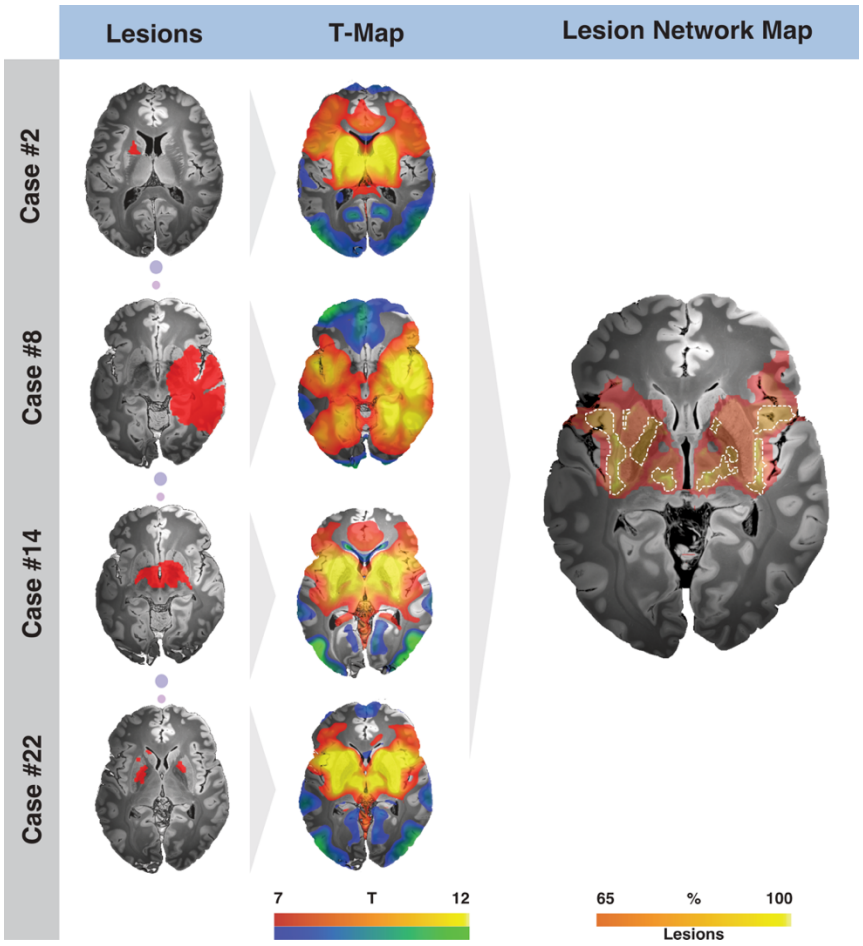

Figure 2 Exemplary cases illustrating the methodological steps used to create the lesion network map. Each lesion mask (left column) extracted from the literature (n = 22) served as a seed region using normative rs-fMRI connectivity data acquired in 1,000 healthy participants. The resulting connectivity profiles (in form of T-maps aggregated across the 1,000 rs-fMRI scans) were then thresholded and summed to identify regions connected to most tic-inducing lesions (right column). The final lesion network map features brain regions connected to voxels encompassed by at least 19 of the 22 identified patient-specific lesion maps.

Although tic-inducing brain lesions expressed spatial heterogeneity, they mapped to a common functional brain network (Fig. 2 and 3). Namely, voxels within a network comprising the insular cortices, cingulate gyrus, striatum, GPi, thalami, and the cerebellum were connected to a majority of lesions (please refer to Fig. 3 and Table 1). This included thalamic and pallidal DBS targets (see insets in Fig. 3).

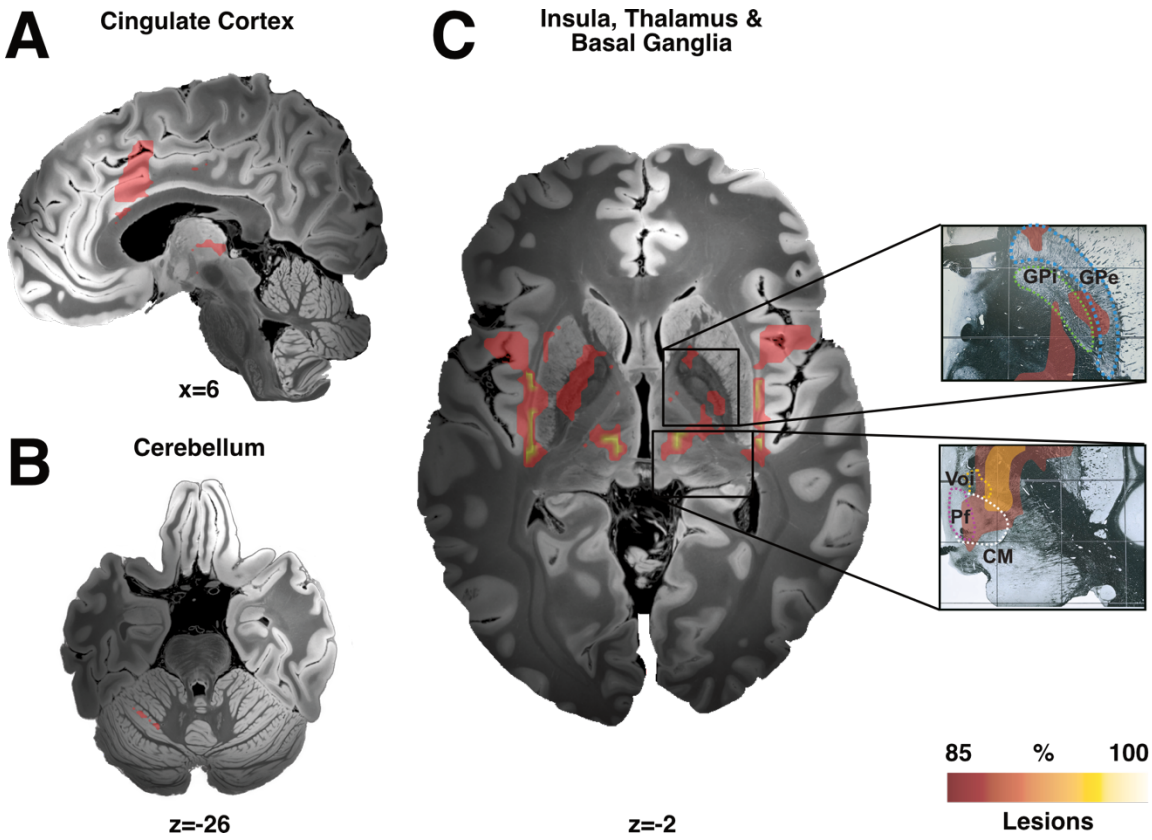

Figure 3 Tic-inducing lesion network map. Lesion network mapping highlighted different cortical and subcortical regions including cingulate cortex (**A**), cerebellum (lobule VI) (**B**), insula, thalamus, striatum, and the pallidum (**C**). Of note, main DBS neuroanatomical targets (GPi and CM-Pf) used to treat primary tic-syndrome are included within the network. CM, centromedian nucleus of thalamus; GPe, globus pallidus externus; GPi, globus pallidus internus; Pf, parafascicular nucleus of thalamus; Voi, ventralis oralis nucleus of thalamus.

However, while the identified network seemed sensitive to tic-inducing lesions, it did not provide insights into how specific it would be to tics. In other words, while spontaneously occurring lesions associated with tics formed part of the network, this did not preclude lesions associated with different symptoms would not fall into the network, as likely. To account for this, we probed the specificity of the identified network by contrasting tic lesion connectivity maps with connectivity maps seeding from 717 lesions within the Harvard Lesion Repository

that were associated with a wider array of neurological and/or psychiatric symptoms. This showed significantly higher connectivity of tic-inducing (vs. other) lesions to the *anterior striatum* (Fig. 4B). Subsequent conjunction analysis identified voxels that were both sensitive and specific to tics mapped (Fig. 4C).

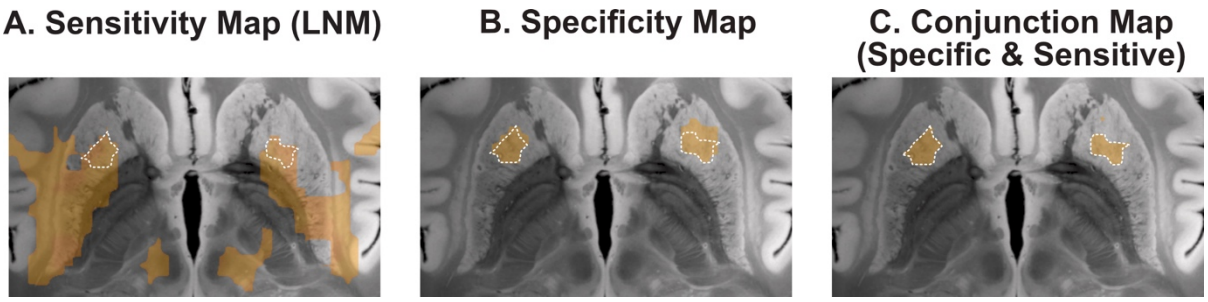

Figure 4 Regions connected to tic-inducing lesions – sensitivity and specificity analysis. Lesion network map (LNM; **A**) represents voxels that were connected to tic-inducing lesions. *Specificity* of connectivity to lesions associated with occurrence of tics was calculated by contrasting connectivity profiles of lesions associated with tics to a total of 717 lesions from the Harvard Lesion Repository (**B**). This analysis highlighted a region within the anterior striatum that would be *specifically* linked to tic-occurrence. Voxels that were *both specific and sensitive* to tic occurrence are demonstrated in **C**. This conjunction map contained voxels that were shown in *both* panels **A** and **B**.

To probe the predictive utility and therapeutic significance of the identified tic-inducing network, we calculated connectivity between DBS stimulation sites in 30 patients with Tourette disorder (Fig. 5) and the lesion network. Connectivity strength correlated with respective tic improvements in both pallidal and thalamic cohorts when analysed together (R = 0.45 at P = 0.01) and each DBS target separately (thalamic target: R = 0.54 at P = 0.01; GPi target: R = 0.45 at P = 0.04; Fig. 6). Connectivity between DBS stimulation sites and the specific map (anterior striatum) and the conjunction map also correlated with clinical improvements (R = 0.43 at P = 0.004, R = 0.43 at P = 0.006; Fig. 6B).

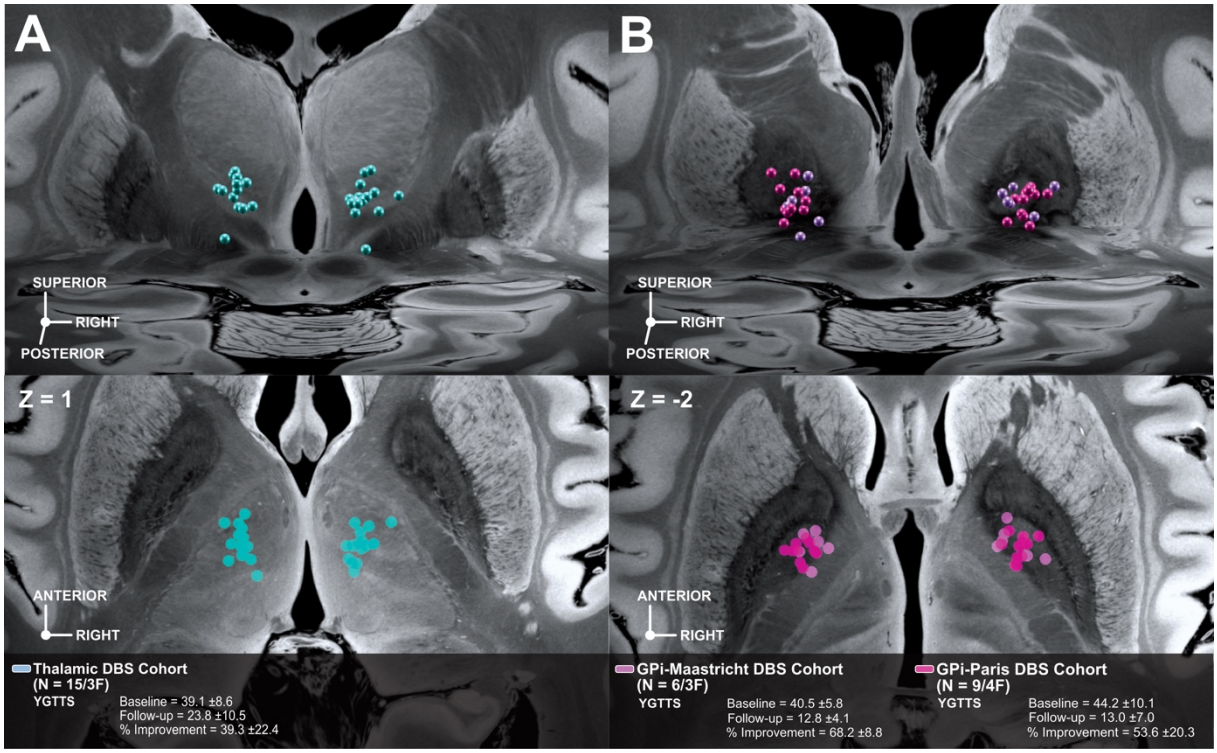

Figure 5 DBS cohorts electrode placement. Each DBS cohort comprises bilaterally implanted electrodes targeting different subcortical region. The thalamic DBS cohort (**A**) consisted of *n* = 15 patients from Cologne clinical center while the GPi cohort (**B**) consisted of 6 patients from Maastricht and 9 from Paris clinical centres. Panels show active contact locations relative to anatomical planes defined by the 100µm postmortem ultra-high resolution postmortem template in an oblique 3D view from posterodorsal (top) and axial slice (bottom) view (where contact sites were orthogonally projected to the plane) [58].

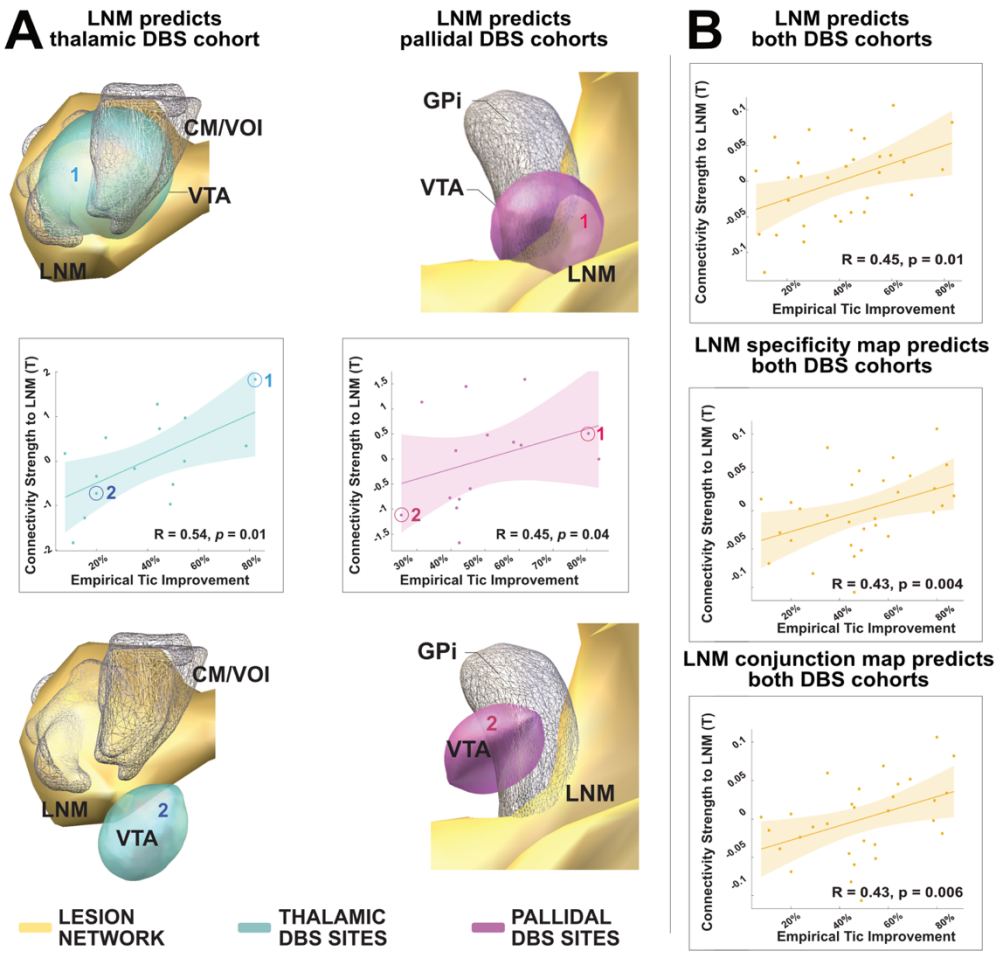

Figure 6 DBS associated tic improvement associates with connectivity to the lesion network map. (**A**) Postoperative percentage improvement of primary tic syndrome from 3 clinical centres (Cologne-thalamic DBS cohort/turquoise and Paris and Maastricht-GPi DBS cohort/magenta) associated with the degree of connectivity between either the thalamic and GPi DBS stimulation sites and the lesion network map. Four example cases of optimal and poor improvements are shown, each demonstrating strong or weak functional connectivity between the DBS site and the lesion network map, respectively. The lesion network map is shown in yellow, and thalamic stimulation sites in cyan, pallidal ones in purple. Respective example cases are marked in scatter plots. (**B**) Correlation plots between the degree of connectivity of the entire patient cohort and the lesion network map (upper panel), the sensitivity map (middle panel), and the conjunction map (lower panel) respectively. CM/VOI, centromedian

nucleus/ventro-oralis nucleus of thalamus; GPi, globus pallidus internus; LNM, lesion network map.

In a final analysis, we wanted to probe optimal DBS connectivity profiles in a data-driven fashion. We did so by correlating connectivity values with clinical improvements for each cohort, in a voxel-wise fashion (following the approach of Horn et al. [42]). This resulted in a set of connections with differences and similarities for the pallidal and thalamic DBS sites. While some sites of optimal connectivity agreed between DBS sites, the two maps were largely different (Fig. 7). However, when probing which regions had positive associations with clinical outcomes *for both sites* (thalamic and pallidal DBS), this carved out a network that included a highly similar pattern of regions as did the lesion network (Fig. 7 and Table 1). Hence, by pinpointing the sites of optimal connectivity for effective DBS *from two DBS targets*, a more specific network emerged that matched the one defined by tic-inducing brain lesions.

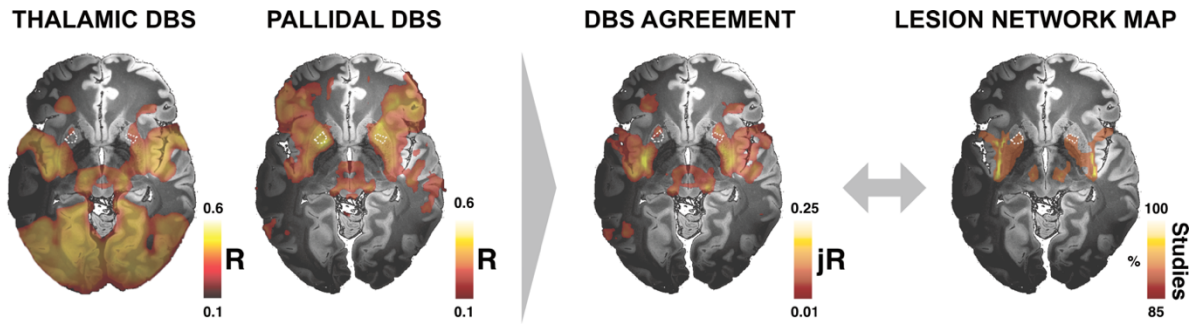

Figure 7 Agreement between DBS and lesion-informed mapping.

In a final data-driven analysis, functional connectivity between DBS targets and all other brain areas that correlated with optimal clinical improvement was separately calculated for the thalamic and pallidal cohorts. This led to different connectivity profiles but also included overlapping regions. These are shown as dashed lines in the two maps and by the agreement map. In the agreement map, only regions with positive association in *both* targets were retained.

This analysis identified a highly similar set of regions as did the lesion network map (also see Table 1).

Discussion

Three major conclusions can be drawn from this study. First, our results confirm that a network of brain regions is involved in tic generation. Second, we show that a sub-region of the anterior striatum shows specificity to tics when comparing lesion network results to a larger database of lesions associated with other neurological and/or psychiatric symptoms. Third, the identified network was able to predict outcomes following DBS in cohorts with two subcortical stimulation targets.

A tic-inducing neural network

Contemporary neurology and neuropsychiatry in part explain pathological changes of behavior as a result of damage to distributed brain networks rather than to isolated brain regions [35]. In this sense, behavioral brain network disorders have been described as 'circuitopathies' or 'connectopathies' [59,60]. In the rare cases of lesion-induced tics identified by our systematic search, the inciting lesions were connected to a common neural circuit, which encompassed structures of the cortico-basal-ganglia-thalamo-cortical circuit, as well as the insular and anterior cingulate cortex (ACC). These regions have previously been implicated in the pathophysiology of tic disorders[23]. For example, in their seminal fMRI study on the neural correlates of tics, Bohlhalter et al. identified a network that preceded tic onset which largely overlapped with the present network, including the insular cortex, ACC, putamen, and thalamus [31]. The relevance of these structures was confirmed in a subsequent study, which employed a similar design with careful time-locked monitoring of tics, providing further support to their involvement in tic occurrence [32]. Moreover, the insular cortex and the ACC have also been associated with specific pathophysiologic aspects of tic occurrence, including premonitory

urges [33] and vocalizations [61]. Of note, the role of the input and output structures of the basal ganglia in tic emergence had already been highlighted by pioneering neuropathological studies in the field [5,6,62] and Hassler's and Dieckman's early neurosurgical therapeutic interventions for tics and obsessive-compulsive symptoms[7]. Indeed, the thalamic and GPi clusters of the network we have identified precisely matched the ablational lesion locations probed by these pioneering studies and showed overlap with the common DBS targets used for the treatment of Tourette disorder (which were inspired by them).[63]

Finally, the network associated with tics identified here covers the claustrum, which could be of potential interest. While the function of the claustrum remains somewhat elusive (and it has been seen as an additional cortical layer by some authors [64]), lesion network mapping has associated a specific part of the claustrum with the occurrence of lesion-induced Parkinsonism[38]. Similar to all parts of the basal ganglia, the claustrum is a widespread structure with inputs and outputs from and to various cortical regions, including connecting the anterior insula with the ACC [65]. Hence, specific parts of the structure could be involved in motor processing (and potentially the occurrence of tics), while others are involved in cognitive or limbic processes

A specific role for the anterior striatum in tic induction

The comparison between individual tic lesion network profiles and a large database of cases with lesions associated with neurological and psychiatric disorders revealed a specific role of the anterior striatum in tic induction, which was identified as a subset of the tic-related lesion network. Conjunction analysis identified a region within the anterior putamen, which was both sensitive and specific to tics. This region mapped to the associative-limbic functional zone of the striatum[66], well within the projection site of CM-Voi. Importantly, this pre-commissural sub-region of the putamen constitutes a complex information processing hub, driven by its

exceptional level of input heterogeneity [67]. Similarly, CM-Voi nuclei receive input from and diffusely project to the entire cerebral cortex [68]. A compelling pathological study of brains of adults with Tourette disorder reported pronounced decreases of different interneuronal populations in the associative and, to a lesser degree, sensorimotor striatum [6]. At the same time, animal models of pharmacologically-induced GABAergic disinhibition within this sub-region of the striatum led to tic-like behaviors [69,70]. This body of pathological and behavioural animal model data suggests that information processing within this striatal hub, and its functional connectivity with other subcortical structures, could be altered in primary tic disorders.

A tic-lesion network as a potential target for neuromodulation

Tic disorders are characterized by clinical heterogeneity and variability in treatment response, including response to DBS [63]. According to a recent estimate, about 30% of adults with Tourette disorder and moderate to severe tics are refractory to non-invasive interventions, and would be eligible for DBS. In the United States alone, this corresponds to more than 6,000 individuals[71]. However, robust predictors of treatment outcome following DBS have not yet been established, motivating the application of both the lesion and DBS network mapping approaches in the present study. Indeed, combining the two methods (as done here) allowed to predict clinical outcomes following DBS in the treatment of Parkinson's Disease and Major Depression based on lesions causing parkinsonism [38] and depression [72]. Another study focusing on dystonia [39] demonstrated anatomical overlap between a lesion-based network and the network associated with positive outcome after DBS.

In Tourette disorder, a first study has applied DBS network mapping, before [73], but did not relate DBS network patterns to lesions associated with tics. Furthermore, the study applied normative *structural* (instead of functional) connectivity and hence results may not be directly comparable to ours. In the study, structural connectivity to an extensive array of brain areas was

associated with DBS-related modulation of tic severity, including limbic, associative, and sensorimotor networks. Interestingly, structural connectivity patterns were largely inverse between the pallidal and thalamic stimulation targets. Although a strong connectivity to limbic and associative networks, including the cingulate cortex, caudate and thalamus, predicted post-DBS tic improvement in patients who received GPi stimulation (n = 34), this was not the case for the thalamic stimulation cohort. In the latter group (n = 32), connectivity to primary sensorimotor and parietal-temporal-occipital networks, as well as the putamen, correlated with reduction in tic severity. In part, this matches with our results which showed different optimal connectivity profiles for both pallidal and thalamic target sites – however, here, networks were not inverse to each other, and their common denominator set of regions precisely matched the network identified by lesions. Crucially, structural connectivity analyses as carried out in the aforementioned study [73] cannot detect indirect (i.e., polysynaptic) connections. In our sample, *functional* connectivity of both pallidal and thalamic cohorts to the same tic-related lesion network was associated with greater tic improvement. Moreover, while in a data-driven analysis of DBS sites, the two optimal connectivity profiles between pallidal and thalamic targets differed, their agreement mapped exactly to the network identified by the lesion analysis. First, these results validate the significance of the tic lesion network in the pathophysiology of tic generation. Second, they provide a functional network template that could inform effective neuromodulatory interventions aimed at reducing tics.

Limitations

Some noteworthy limitations apply to this study. First, both literature-derived network maps and DBS cases were acquired retrospectively. In the former, causality between brain lesions and occurrence of tics cannot be established with absolute certainty. This has been a longstanding limitation of studying case reports across symptoms and constitutes a true limitation. However, lesions resulting in the emergence of tics are rare and from 22 identified

cases, 19 mapped to a shared network. We manually segmented lesion locations on the MNI template, resulting in 2D regions. Prior analyses showed that this would lead to similar connectivity profiles as corresponding 3D lesions [74,75] and the same procedure has been carried out in several lesion network mapping studies that showed robust findings [38,41,72]. Prospective validation of network maps to explain variance in clinical outcome will be crucial to move forward.

Second, we carried out network mapping for both lesions and DBS cases using normative functional connectivity acquired in healthy individuals. This has been done successfully in previous studies yielding results that were used to cross-predict clinical improvement in independent cohorts in a variety of diseases [42-46,57,59]. At the same time, this approach applies a "broad lens" view on human brain function and may not reveal patient- or disease-specific details of brain connectivity. The method determines the networks underlying DBS sites or lesions *within the average healthy human brain*. This notion is crucial when interpreting results but indeed has multiple practical advantages: for instance, lesions (with ischemic tissue) would not show patient-specific network connectivity, even if patient-specific functional scans were available (since the lesion site is not active after stroke). In other words, functional connectivity from stroke sites is not present and cannot be calculated using patient-specific fMRI data. In both stroke and DBS, distributed brain networks would be *altered by* the incidents (infarction or neurostimulation) themselves. Here, we ask which networks of the *pre*-stroke / *pre*-DBS brain would be affected by both incidents and argue that this would identify exactly the networks with therapeutic value.

Third, the process of DBS electrode reconstruction is prone to inaccuracies that can be relevant, as previously discussed [53]. Moreover, the model applied to estimate stimulation volumes surrounding DBS electrodes applied here may be over-simplistic compared to more elaborate methods [76-78]. However, in the context of fMRI mapping (with an isotropic resolution of 2 mm),

subtle inaccuracies of the applied model may not be as impactful as in more fine-grained analyses.

Finally, we note that while both lesions and DBS sites identified a share network with high spatial overlap, lesions that fell into the network induced tics while DBS to the network alleviated tics. With the methods at hand, we may currently only speculate why that is the case. For one, we believe that the disruption of the network is involved in producing tics and such a disruption could be induced by lesions that corrupt the functionality of the network. How exactly this "disruption" is mechanistically implemented cannot be investigated with the methods of the present study, but local field potential recordings from both thalamic and pallidal DBS electrodes showed that prolonged theta bursts in both targets were associated with preoperative motor tic severity[16]. In other diseases such as PD and dystonia, DBS is known to tone down such aberrant elevated network activity [79]. Hence, our current working model constitutes that lesions (or other etiologies) could lead to network dysfunction (including the occurrence of noisy feedback carrier signals [80,81]) and DBS could in turn selectively tone down / compensate these aberrant signals, freeing up bandwidth for physiological communication within the network to happen again.

Conclusions

This study could associate a functional network including striatal, thalamic, and insular regions of the human brain with i) the occurrence of tics resulting from brain lesions and ii) successful tic reduction following DBS treatment. We could demonstrate that the connectivity between DBS electrodes implanted in two different target sites and our network identified by tic-inducing lesions was able to predict significant amounts of variance in tic improvements. In a

data-driven approach, the regions associated with improvement following *both* pallidal and thalamic DBS mapped to the exact same set of regions identified by the lesion network analysis.

Funding

CG is supported by a Freigeist Fellowship of the VolkswagenStiftung. He has received honoraria for educational activities from the Movement Disorder Society. He has served as ad hoc advisory board to Biomarin Pharmaceutical and Lundbeck.

JCB and VVV are funded by the Deutsche Forschungsgemeinschaft (DFG, German Research Foundation) – Project-ID 431549029 – SFB 1451.

AFL receives royalties from 'Springer Media' and 'De Tijdstroom' Publishers.

MDF was supported by the Nancy Lurie Marks Foundation, the Kaye Family Research Endowment, the Ellison / Baszucki Foundation, and the NIH (R01MH113929, R21MH126271, R56AG069086, R01MH115949, and R01AG060987).

AKK is a consultant to Boston Scientific and has received honoraria for speaking from Medtronic, Boston Scientific, and Abbott, also grants from Medtronic, all outside the submitted work.

A.H. was supported by the German Research Foundation (Deutsche Forschungsgemeinschaft, Emmy Noether Stipend 410169619 and 424778381 – TRR 295) as well as Deutsches Zentrum für Luft- und Raumfahrt (DynaSti grant within the EU Joint Programme Neurodegenerative Disease Research, JPND). A.H. is participant in the BIH-Charité Clinician Scientist Program funded by the Charité –Universitätsmedizin Berlin and the Berlin Institute of Health. He also reports lecture fees by Boston Scientific unrelated to present work.

BAF, JFF, CH, CN, DM, JL, TB, LA, NP and YW report no relevant funding for this work.

Competing Interests

The authors report no competing interests.

Supplementary material

Supplementary material is available at *Brain* online.

Table 1 Peak coordinates. Table summarizes MNI coordinates of regions visualized on different brain connectivity maps presented in the study (Fig. 3 and 7).

Region	Hemisphere	Thalamus R-Map X/Y/Z (R-Value)	GPi R-Map X/Y/Z (R-Value)	Agreement R-Map X/Y/Z (R-Value)	Lesion Network Map X/Y/Z (T-Value)
Sub-lobar insula (BA13)	LH	-42/-8/2 (0.66)	-34/-28/14 (0.45)	-34/-28/14 (0.28)	-44/10/-8 (20)
	RH	46/-6/0 (0.67)	42/-18/14 (0.48)	46/-16/10 (0.27)	44/12/-8 (19)
Putamen	LH	-32/-14/-2 (0.68)	-18/6/-6 (0.63)	-30/-6/-8 (0.25)	-20/4/-14 (20)
	RH	34/-18/6 (0.64)	24/4/-10 (0.59)	32/-12/12 (0.20)	20/4/-14 (20)
Cingulate Gyrus (limbic lobe)	LH	-6/-6/40 (0.63)	-4/-2/34 (0.64)	0/-10/42 (0.31)	0/12/24 (19)
	RH	4/-14/44 (0.65)	4/-2/34 (0.55)	2/-12/42 (0.27)	10/22/24 (19)
Precentral Gyrus	LH	-66/0/10 (0.66)	-68/0/26 (0.46)	-68/0/26 (0.26)	-42/12/2 (19)
	RH	70/4/6 (0.67)	44/18/34 (0.63)	70/6/4 (0.30)	44/8/2 (19)
Mammillary Body	LH	-10/-16/-2 (0.77)	-8/-20/-2 (0.08)	-10/-16/-2 (0.06)	-8/-20/-2 (20)
	RH	12/-20/0 (0.57)	12/-22/-2 (0.04)	12/-22/-2 (0.02)	12/-16/-2 (20)
Midbrain	LH	-8/-16/-4 (0.71)	0/-34/0 (0.44)	-6/-30/0 (0.12)	-8/-22/-4 (20)
	RH	16/-22/-4 (0.62)	2/-34/0 (0.53)	16/-26/-4 (0.17)	10/-22/-4 (20)
Medial Dorsal Nucleus	LH	-10/-18/4 (0.62)	-4/-12/8 (0.58)	-4/-14/6 (0.27)	-6/-20/2 (20)
	RH	14/-20/4 (0.58)	4/-14/10 (0.57)	4/-12/4 (0.25)	8/-20/2 (20)
Ventral Posterior Medial Nucleus	LH	-14/-18/-2 (0.68)	-14/-18/8 (0.17)	-14/-18/8 (0.08)	-16/-22/4 (20)
	RH	18/-20/-2 (0.62)	20/-20/8 (0.26)	18/-20/8 (0.13)	18/-22/6 (20)
Cingulate Gyrus (BA24)	LH	-10/-4/40 (0.64)	-2/0/34 (0.65)	-4/-14/40 (0.34)	-2/12/24 (19)
	RH	12/-4/40 (0.64)	4/0/34 (0.59)	4/0/34 (0.27)	8/14/24 (19)
Claustrum	LH	-36/-22/4 (0.65)	-28/6/12 (0.47)	-34/-24/8 (0.21)	-38/-20/-8 (20)
	RH	38/-20/4 (0.65)	34/-14/14 (0.44)	34/-14/14 (0.25)	38/-14/-10 (20)
Pulvinar	LH	-20/-24/2 (0.65)	-6/-28/4 (0.40)	-10/-24/12 (0.17)	-18/-24/4 (20)
	RH	20/-28/2 (0.60)	12/-26/12 (0.30)	20/-22/14 (0.15)	20/-24/6 (20)
Inferior Frontal Gyrus	LH	-64/12/12 (0.66)	-60/22/26 (0.52)	-64/10/26 (0.22)	-48/14/-10 (19)
	RH	68/10/12 (0.61)	62/30/-4 (0.59)	68/14/24 (0.28)	50/16/-6 (19)
Globus Pallidus, pars externa	LH	-26/-16/0 (0.48)	-14/6/-2 (0.48)	-26/-18/0 (0.08)	-20/-4/-10 (19)
	RH	30/-12/-2 (0.50)	22/2/-8 (0.50)	30/-14/-6 (0.14)	18/4/-10 (20)
Globus Pallidus, pars interna	LH	-18/-10/0 (0.28)	-12/2/-2 (0.17)	-20/-10/-6 (0)	-16/-8/-10 (0)
	RH	24/-14/-4 (0.32)	16/-2/-6 (0.18)	24/-12/-6 (0.02)	18/-2/-10 (19)

References

1. Kurvits L, Martino D, Ganos C. Clinical Features That Evoke the Concept of Disinhibition in Tourette Syndrome. *Front Psychiatry*. 2020;11:21. doi:10.3389/fpsyt.2020.00021
2. Ganos C, Roessner V, Munchau A. The functional anatomy of Gilles de la Tourette syndrome. *Neurosci Biobehav Rev*. Jul 2013;37:1050-62.doi:10.1016/j.neubiorev.2012.11.004
3. Hashemiyoon R, Kuhn J, Visser-Vandewalle V. Putting the Pieces Together in Gilles de la Tourette Syndrome: Exploring the Link Between Clinical Observations and the Biological Basis of Dysfunction. *Brain topography*. Jan 2017;30:3-29. doi:10.1007/s10548-016-0525-z
4. Mink JW. Basal ganglia dysfunction in Tourette's syndrome: a new hypothesis. Research Support, Non-U.S. Gov't Research Support, U.S. Gov't, P.H.S. Review. *Pediatr Neurol*. Sep 2001;25:190-8.

5. Kalanithi PS, Zheng W, Kataoka Y, et al. Altered parvalbumin-positive neuron distribution in basal ganglia of individuals with Tourette syndrome. Research Support, N.I.H., Extramural Research Support, Non-U.S. Gov't Research Support, U.S. Gov't, P.H.S. *Proc Natl Acad Sci U S A*. Sep 13 2005;102:13307-12. doi:10.1073/pnas.0502624102

6. Kataoka Y, Kalanithi PS, Grantz H, et al. Decreased number of parvalbumin and cholinergic interneurons in the striatum of individuals with Tourette syndrome. Research Support, N.I.H., Extramural Research Support, Non-U.S. Gov't. *J Comp Neurol*. Feb 1 2010;518:277-91. doi:10.1002/cne.22206

7. Hassler R, Dieckmann G. [Stereotaxic treatment of tics and inarticulate cries or coprolalia considered as motor obsessional phenomena in Gilles de la Tourette's disease]. *Rev Neurol (Paris)*. Aug 1970;123:89-100. Traitement stereotaxique des tics et cris inarticules ou coprolaliques consideres comme phenomene d'obsession motrice au cours de la maladie de Gilles de la Tourette.
8. Vandewalle V, van der Linden C, Groenewegen HJ, Caemaert J. Stereotactic treatment of Gilles de la Tourette syndrome by high frequency stimulation of thalamus. 10.1016/S0140-6736(98)05964-9. *The Lancet*. 1999;353:724. doi:papers3://publication/doi/10.1016/S0140-6736(98)05964-9
9. Ackermans L, Duits A, van der Linden C, et al. Double-blind clinical trial of thalamic stimulation in patients with Tourette syndrome. Randomized Controlled Trial. *Brain*. Mar 2011;134(Pt 3):832-44. doi:10.1093/brain/awq380
10. Baldermann JC, Kuhn J, Schuller T, et al. Thalamic deep brain stimulation for Tourette Syndrome: A naturalistic trial with brief randomized, double-blinded sham-controlled periods. *Brain Stimul*. Jul 7 2021;14:1059-1067. doi:10.1016/j.brs.2021.07.003
11. Baldermann JC, Hennen C, Schüller T, et al. A functional network target for tic reduction during thalamic stimulation for Tourette Syndrome. *bioRxiv*. 2021:2021.08.27.457924. doi:10.1101/2021.08.27.457924
12. Huys D, Bartsch C, Koester P, et al. Motor Improvement and Emotional Stabilization in Patients With Tourette Syndrome After Deep Brain Stimulation of the Ventral Anterior and Ventrolateral Motor Part of the Thalamus. *Biol Psychiatry*. Mar 1 2016;79:392-401. doi:10.1016/j.biopsych.2014.05.014
13. Kefalopoulou Z, Zrinzo L, Jahanshahi M, et al. Bilateral globus pallidus stimulation for severe Tourette's syndrome: a double-blind, randomised crossover trial. *The Lancet Neurology*. Jun 2015;14:595-605. doi:10.1016/S1474-4422(15)00008-3

14. Welter ML, Houeto JL, Thobois S, et al. Anterior pallidal deep brain stimulation for Tourette's syndrome: a randomised, double-blind, controlled trial. *The Lancet Neurology*. Aug 2017;16:610-619. doi:10.1016/S1474-4422(17)30160-6
15. Martinez-Ramirez D, Jimenez-Shahed J, Leckman JF, et al. Efficacy and Safety of Deep Brain Stimulation in Tourette Syndrome: The International Tourette Syndrome Deep Brain Stimulation Public Database and Registry. *JAMA Neurol*. Mar 1 2018;75:353-359. doi:10.1001/jamaneurol.2017.4317
16. Neumann WJ, Huebl J, Brucke C, et al. Pallidal and thalamic neural oscillatory patterns in tourette's syndrome. *Ann Neurol*. Oct 2018;84:505-514. doi:10.1002/ana.25311
17. Cagle JN, Okun MS, Opri E, et al. Differentiating tic electrophysiology from voluntary movement in the human thalamocortical circuit. *J Neurol Neurosurg Psychiatry*. May 2020;91:533-539. doi:10.1136/jnnp-2019-321973
18. Priori A, Giannicola G, Rosa M, et al. Deep brain electrophysiological recordings provide clues to the pathophysiology of Tourette syndrome. *Neurosci Biobehav Rev*. Jul 2013;37:1063-8. doi:10.1016/j.neubiorev.2013.01.011
19. Karp BI, Porter S, Toro C, Hallett M. Simple motor tics may be preceded by a premotor potential. *J Neurol Neurosurg Psychiatry*. Jul 1996;61:103-6.
20. van der Salm SM, Tijssen MA, Koelman JH, van Rootselaar AF. The bereitschaftspotential in jerky movement disorders. Research Support, Non-U.S. Gov't. *J Neurol Neurosurg Psychiatry*. Dec 2012;83:1162-7. doi:10.1136/jnnp-2012-303081
21. Orth M, Munchau A, Rothwell JC. Corticospinal system excitability at rest is associated with tic severity in tourette syndrome. *Biol Psychiatry*. Aug 01 2008;64:248-51. doi:10.1016/j.biopsych.2007.12.009
22. Franzkowiak S, Pollok B, Biermann-Ruben K, et al. Motor-cortical interaction in Gilles de la Tourette syndrome. Research Support, Non-U.S. Gov't. *PLoS One*. 2012;7:e27850. doi:10.1371/journal.pone.0027850
23. Martino D, Ganos C, Worbe Y. Neuroimaging Applications in Tourette's Syndrome. *Int Rev Neurobiol*. 2018;143:65-108. doi:10.1016/bs.irn.2018.09.008
24. Worbe Y, Gerardin E, Hartmann A, et al. Distinct structural changes underpin clinical phenotypes in patients with Gilles de la Tourette syndrome. Research Support, Non-U.S. Gov't. *Brain*. Dec 2010;133(Pt 12):3649-60. doi:10.1093/brain/awq293
25. Draganski B, Martino D, Cavanna AE, et al. Multispectral brain morphometry in Tourette syndrome persisting into adulthood. Research Support, Non-U.S. Gov't. *Brain*. Dec 2010;133(Pt 12):3661-75. doi:10.1093/brain/awq300
26. Liu Y, Miao W, Wang J, et al. Structural abnormalities in early Tourette syndrome children: a combined voxel-based morphometry and tract-based spatial statistics study. *PLoS One*. 2013;8:e76105. doi:10.1371/journal.pone.0076105
27. Draper A, Jackson GM, Morgan PS, Jackson SR. Premonitory urges are associated with decreased grey matter thickness within the insula and sensorimotor cortex in young people with Tourette syndrome. *J Neuropsychol*. Mar 2016;10:143-53. doi:10.1111/jnp.12089
28. Thomalla G, Siebner HR, Jonas M, et al. Structural changes in the somatosensory system correlate with tic severity in Gilles de la Tourette syndrome. Multicenter Study Research Support, Non-U.S. Gov't. *Brain*. Mar 2009;132(Pt 3):765-77. doi:10.1093/brain/awn339

29. Fahim C, Yoon U, Das S, et al. Somatosensory-motor bodily representation cortical thinning in Tourette: effects of tic severity, age and gender. Research Support, Non-U.S. Gov't. *Cortex*. Jun 2010;46:750-60. doi:10.1016/j.cortex.2009.06.008
30. Sowell ER, Kan E, Yoshii J, et al. Thinning of sensorimotor cortices in children with Tourette syndrome. Research Support, N.I.H., Extramural. *Nat Neurosci*. Jun 2008;11:637-9. doi:10.1038/nn.2121

31. Bohlhalter S, Goldfine A, Matteson S, et al. Neural correlates of tic generation in Tourette syndrome: an event-related functional MRI study. *Brain*. Aug 2006;129(Pt 8):2029-37. doi:10.1093/brain/awl050
32. Neuner I, Werner CJ, Arrubla J, et al. Imaging the where and when of tic generation and resting state networks in adult Tourette patients. *Front Hum Neurosci*. 2014;8:362. doi:10.3389/fnhum.2014.00362
33. Tinaz S, Malone P, Hallett M, Horovitz SG. Role of the right dorsal anterior insula in the urge to tic in Tourette syndrome. *Mov Disord*. Aug 2015;30:1190-7. doi:10.1002/mds.26230
34. Worbe Y, Sgambato-Faure V, Epinat J, et al. Towards a primate model of Gilles de la Tourette syndrome: anatomo-behavioural correlation of disorders induced by striatal dysfunction. *Cortex*. Apr 2013;49:1126-40. doi:10.1016/j.cortex.2012.08.020
35. Fox MD. Mapping Symptoms to Brain Networks with the Human Connectome. *The New England journal of medicine*. Dec 6 2018;379:2237-2245. doi:10.1056/NEJMra1706158
36. Boes AD, Prasad S, Liu H, et al. Network localization of neurological symptoms from focal brain lesions. *Brain*. Oct 2015;138(Pt 10):3061-75. doi:10.1093/brain/awv228
37. Laganiere S, Boes AD, Fox MD. Network localization of hemichorea-hemiballismus. *Neurology*. Jun 7 2016;86:2187-95. doi:10.1212/WNL.0000000000002741
38. Joutsa J, Horn A, Hsu J, Fox MD. Localizing parkinsonism based on focal brain lesions. *Brain*. Aug 1 2018;141:2445-2456. doi:10.1093/brain/awy161
39. Corp DT, Joutsa J, Darby RR, et al. Network localization of cervical dystonia based on causal brain lesions. *Brain*. Jun 1 2019;142:1660-1674. doi:10.1093/brain/awz112
40. Darby RR, Joutsa J, Burke MJ, Fox MD. Lesion network localization of free will. *Proc Natl Acad Sci U S A*. Oct 16 2018;115:10792-10797. doi:10.1073/pnas.1814117115
41. Darby RR, Horn A, Cushman F, Fox MD. Lesion network localization of criminal behavior. *Proc Natl Acad Sci U S A*. Jan 16 2018;115:601-606. doi:10.1073/pnas.1706587115
42. Horn A, Reich M, Vorwerk J, et al. Connectivity Predicts deep brain stimulation outcome in Parkinson disease. *Ann Neurol*. Jul 2017;82:67-78. doi:10.1002/ana.24974
43. Irmen F, Horn A, Mosley P, et al. Left Prefrontal Connectivity Links Subthalamic Stimulation with Depressive Symptoms. *Ann Neurol*. Jun 2020;87:962-975. doi:10.1002/ana.25734
44. Al-Fatly B, Ewert S, Kubler D, Kroneberg D, Horn A, Kuhn AA. Connectivity profile of thalamic deep brain stimulation to effectively treat essential tremor. *Brain*. Oct 1 2019;142:3086-3098. doi:10.1093/brain/awz236
45. Baldermann JC, Melzer C, Zapf A, et al. Connectivity Profile Predictive of Effective Deep Brain Stimulation in Obsessive-Compulsive Disorder. *Biol Psychiatry*. May 1 2019;85:735-743. doi:10.1016/j.biopsych.2018.12.019
46. Li N, Baldermann JC, Kibleur A, et al. A unified connectomic target for deep brain stimulation in obsessive-compulsive disorder. *Nat Commun*. Jul 3 2020;11:3364. doi:10.1038/s41467-020-16734-3
47. Siddiqi SH, Schaper F, Horn A, et al. Brain stimulation and brain lesions converge on common causal circuits in neuropsychiatric disease. *Nat Hum Behav*. Jul 8 2021;doi:10.1038/s41562-021-01161-1
48. Horn A, Kuhn AA. Lead-DBS: a toolbox for deep brain stimulation electrode localizations and visualizations. *Neuroimage*. Feb 15 2015;107:127-135. doi:10.1016/j.neuroimage.2014.12.002
49. Holmes AJ, Hollinshead MO, O'Keefe TM, et al. Brain Genomics Superstruct Project initial data release with structural, functional, and behavioral measures. *Sci Data*. 2015;2:150031. doi:10.1038/sdata.2015.31

50. Yeo BT, Krienen FM, Sepulcre J, et al. The organization of the human cerebral cortex estimated by intrinsic functional connectivity. *J Neurophysiol*. Sep 2011;106:1125-65. doi:10.1152/jn.00338.2011
51. Cohen AL, Fox MD. Reply: The influence of sample size and arbitrary statistical thresholds in lesion-network mapping. *Brain*. May 1 2020;143:e41. doi:10.1093/brain/awaa095
52. Eklund A, Nichols TE, Knutsson H. Cluster failure: Why fMRI inferences for spatial extent have inflated false-positive rates. *Proc Natl Acad Sci U S A*. Jul 12 2016;113:7900-5. doi:10.1073/pnas.1602413113
53. Horn A, Li N, Dembek TA, et al. Lead-DBS v2: Towards a comprehensive pipeline for deep brain stimulation imaging. *Neuroimage*. Jan 1 2019;184:293-316. doi:10.1016/j.neuroimage.2018.08.068
54. Avants BB, Epstein CL, Grossman M, Gee JC. Symmetric diffeomorphic image registration with cross-correlation: evaluating automated labeling of elderly and neurodegenerative brain. *Med Image Anal*. Feb 2008;12:26-41. doi:10.1016/j.media.2007.06.004
55. Husch A, M VP, Gemmar P, Goncalves J, Hertel F. PaCER - A fully automated method for electrode trajectory and contact reconstruction in deep brain stimulation. *Neuroimage Clin*. 2018;17:80-89. doi:10.1016/j.nicl.2017.10.004
56. van Albada SJ, Robinson PA. Transformation of arbitrary distributions to the normal distribution with application to EEG test-retest reliability. 10.1016/j.jneumeth.2006.11.004. *J Neurosci Methods*. 2007;161:205-211. doi:papers3://publication/doi/10.1016/j.jneumeth.2006.11.004
57. Li N, Hollunder B, Baldermann JC, et al. A Unified Functional Network Target for Deep Brain Stimulation in Obsessive-Compulsive Disorder. *Biol Psychiatry*. Apr 20 2021;doi:10.1016/j.biopsych.2021.04.006
58. Edlow BL, Mareyam A, Horn A, et al. 7 Tesla MRI of the ex vivo human brain at 100 micron resolution. *Sci Data*. Oct 30 2019;6:244. doi:10.1038/s41597-019-0254-8
59. Horn A, Fox MD. Opportunities of connectomic neuromodulation. *Neuroimage*. Nov 1 2020;221:117180. doi:10.1016/j.neuroimage.2020.117180
60. Lozano AM, Lipsman N. Probing and regulating dysfunctional circuits using deep brain stimulation. *Neuron*. Feb 6 2013;77:406-24. doi:10.1016/j.neuron.2013.01.020
61. McCairn KW, Nagai Y, Hori Y, et al. A Primary Role for Nucleus Accumbens and Related Limbic Network in Vocal Tics. *Neuron*. Jan 20 2016;89:300-7. doi:10.1016/j.neuron.2015.12.025
62. Balthasar K. [The anatomical substratum of the generalized tic disease (maladie des tics, Gilles de la Tourette); arrest of development of the corpus striatum]. *Arch Psychiatr Nervenkr Z Gesamte Neurol Psychiatr*. 1957;195:531-49. Uber das anatomische Substrat der generalisierten Tic-Krank-heit (maladie des tics, Gilles de la Tourette): Entwicklungshemmung des corpus striatum. doi:10.1007/BF00343129
63. Johnson KA, Fletcher PT, Servello D, et al. Image-based analysis and long-term clinical outcomes of deep brain stimulation for Tourette syndrome: a multisite study. *J Neurol Neurosurg Psychiatry*. Oct 2019;90:1078-1090. doi:10.1136/jnnp-2019-320379
64. Swanson LW. Cerebral hemisphere regulation of motivated behavior. *Brain Res*. Dec 15 2000;886:113-164. doi:10.1016/s0006-8993(00)02905-x
65. Chia Z, Augustine GJ, Silberberg G. Synaptic Connectivity between the Cortex and Claustrum Is Organized into Functional Modules. *Curr Biol*. Jul 20 2020;30:2777-2790 e4. doi:10.1016/j.cub.2020.05.031
66. Choi EY, Yeo BTT, Buckner RL. The organization of the human striatum estimated by intrinsic functional connectivity. 10.1152/jn.00270.2012. *J Neurophysiol*. 2012;108:2242-2263. doi:papers3://publication/doi/10.1152/jn.00270.2012

67. McCutcheon RA, Abi-Dargham A, Howes OD. Schizophrenia, Dopamine and the Striatum: From Biology to Symptoms. *Trends Neurosci*. Mar 2019;42:205-220. doi:10.1016/j.tins.2018.12.004
68. Nieuwenhuys R, Voogd J, Huijzen Cv. *The human central nervous system*. 4th ed. Springer; 2008:xiv, 967 p.
69. McCairn KW, Iriki A, Isoda M. Global dysrhythmia of cerebro-basal ganglia-cerebellar networks underlies motor tics following striatal disinhibition. *J Neurosci*. Jan 9 2013;33:697-708. doi:10.1523/JNEUROSCI.4018-12.2013
70. Tremblay L, Worbe Y, Thobois S, Sgambato-Faure V, Feger J. Selective dysfunction of basal ganglia subterritories: From movement to behavioral disorders. *Mov Disord*. Aug 2015;30:1155-70. doi:10.1002/mds.26199
71. Martino D, Deeb W, Jimenez-Shahed J, et al. The 5 Pillars in Tourette Syndrome Deep Brain Stimulation Patient Selection: Present and Future. *Neurology*. Apr 6 2021;96:664-676. doi:10.1212/WNL.0000000000011704
72. Padmanabhan JL, Cooke D, Joutsa J, et al. A Human Depression Circuit Derived From Focal Brain Lesions. *Biol Psychiatry*. Nov 15 2019;86:749-758. doi:10.1016/j.biopsych.2019.07.023
73. Johnson KA, Duffley G, Anderson DN, et al. Structural connectivity predicts clinical outcomes of deep brain stimulation for Tourette syndrome. *Brain*. Aug 1 2020;143:2607-2623. doi:10.1093/brain/awaa188
74. Darby R, Laganiere S, Pascual-Leone A, Prasad S, Fox MD. Finding the imposter: brain connectivity of lesions causing delusional misidentifications. 10.1093/brain/aww288. *Brain*. 2016:1-11. doi:papers3://publication/doi/10.1093/brain/aww288
75. Boes AD, Prasad S, Liu H, et al. Network localization of neurological symptoms from focal brain lesions. 10.1093/brain/awv228. *Brain*. 2015;138:3061-3075. doi:papers3://publication/doi/10.1093/brain/awv228
76. Gunalan K, Chaturvedi A, Howell B, et al. Creating and parameterizing patient-specific deep brain stimulation pathway-activation models using the hyperdirect pathway as an example. *PLoS One*. 2017;12:e0176132. doi:10.1371/journal.pone.0176132
77. Duffley G, Anderson DN, Vorwerk J, Dorval AD, Butson CR. Evaluation of methodologies for computing the deep brain stimulation volume of tissue activated. *J Neural Eng*. Oct 29 2019;16:066024. doi:10.1088/1741-2552/ab3c95
78. Howell B, Gunalan K, McIntyre CC. A Driving-Force Predictor for Estimating Pathway Activation in Patient-Specific Models of Deep Brain Stimulation. *Neuromodulation*. Jun 2019;22:403-415. doi:10.1111/ner.12929
79. Kuhn AA, Volkmann J. Innovations in deep brain stimulation methodology. *Mov Disord*. Jan 2017;32:11-19. doi:10.1002/mds.26703
80. Horn A, Al-Fatly B, Neumann WJ, Neudorfer C. Chapter 1 - Connectomic DBS: An introduction. In: Horn A, ed. *Connectomic Deep Brain Stimulation*. Academic Press; 2022:3-23.
81. Brown P. Oscillatory nature of human basal ganglia activity: relationship to the pathophysiology of Parkinson's disease. *Mov Disord*. Apr 2003;18(4):357-63. doi:10.1002/mds.10358

Figure Legends

Figure 1 Tic-inducing lesions. The spatial distribution of lesion masks extracted from 22 case reports included in the current study mapped to a wide extent of brain regions. All binary masks were drawn in MNI space and visualized on an ultra-high resolution postmortem template for anatomical reference[58].

Figure 2 Exemplary cases illustrating the methodological steps used to create the lesion network map. Each lesion mask (left column) extracted from the literature (n = 22) served as a seed region using normative rs-fMRI connectivity data acquired in 1,000 healthy participants. The resulting connectivity profiles (in form of T-maps aggregated across the 1,000 rs-fMRI scans) were then thresholded and summed to identify regions connected to most tic-inducing lesions (right column). The final lesion network map features brain regions connected to voxels encompassed by at least 19 of the 22 identified patient-specific lesion maps.

Figure 3 Tic-inducing lesion network map. Lesion network mapping highlighted different cortical and subcortical regions including cingulate cortex (**A**), cerebellum (lobule VI) (**B**), insula, thalamus, striatum, and the pallidum (**C**). Of note, main DBS neuroanatomical targets (GPi and CM-Pf) used to treat primary tic-syndrome are included within the network. CM, centromedian nucleus of thalamus; GPe, globus pallidus externus; GPi, globus pallidus internus; Pf, parafascicular nucleus of thalamus; Voi, ventralis oralis nucleus of thalamus.

Figure 4 Regions connected to tic-inducing lesions – sensitivity and specificity analysis. Lesion network map (LNM; **A**) represents voxels that were connected to tic-inducing lesions. *Specificity* of connectivity to lesions associated with occurrence of tics was calculated by contrasting connectivity profiles of lesions associated with tics to a total of 717 lesions from

the Harvard Lesion Repository (**B**). This analysis highlighted a region within the anterior striatum that would be *specifically* linked to tic-occurrence. Voxels that were *both specific and sensitive* to tic occurrence are demonstrated in **C**. This conjunction map contained voxels that were shown in *both* panels **A** and **B**.

Figure 5 DBS cohorts electrode placement. Each DBS cohort comprises bilaterally implanted electrodes targeting different subcortical region. The thalamic DBS cohort (**A**) consisted of n = 15 patients from Cologne clinical center while the GPi cohort (**B**) consisted of 6 patients from Maastricht and 9 from Paris clinical centres. Panels show active contact locations relative to anatomical planes defined by the 100µm postmortem ultra-high resolution postmortem template in an oblique 3D view from posterodorsal (top) and axial slice (bottom) view (where contact sites were orthogonally projected to the plane) [58].

Figure 6 DBS associated tic improvement associates with connectivity to the lesion network map. (**A**) Postoperative percentage improvement of primary tic syndrome from 3 clinical centres (Cologne-thalamic DBS cohort/turquoise and Paris and Maastricht-GPi DBS cohort/magenta) associated with the degree of connectivity between either the thalamic and GPi DBS stimulation sites and the lesion network map. Four example cases of optimal and poor improvements are shown, each demonstrating strong or weak functional connectivity between the DBS site and the lesion network map, respectively. The lesion network map is shown in yellow, and thalamic stimulation sites in cyan, pallidal ones in purple. Respective example cases are marked in scatter plots. (**B**) Correlation plots between the degree of connectivity of the entire patient cohort and the lesion network map (upper panel), the sensitivity map (middle panel), and the conjunction map (lower panel) respectively. CM/VOI, centromedian nucleus/ventro-oralis nucleus of thalamus; GPi, globus pallidus internus; LNM, lesion network map.

Figure 7 Agreement between DBS and lesion-informed mapping.

In a final data-driven analysis, functional connectivity between DBS targets and all other brain areas that correlated with optimal clinical improvement was separately calculated for the thalamic and pallidal cohorts. This led to different connectivity profiles but also included overlapping regions. These are shown as dashed lines in the two maps and by the agreement map. In the agreement map, only regions with positive association in *both* targets were retained.

Supplementary Material

Electronic search strategy:

- Pubmed:
  - Date: 19.03.2020
  - Term: *((Tics/etiology or Tics/pathology or Tourette Syndrome/etiology or Tourette Syndrome/pathology or tic disorders/etiology or Tic disorders/pathology or secondary tics or Tourettis*) AND (brain lesion or brain damage or white matter abnormalities or gray matter abnormalities or brain abnormalities or spinal injur* or spinal lesion* or brain injur* or head injur* or craniocerebral trauma or posttraumatic or post-traumatic or central nervous system infection or wounds and injuries or central nervous system neoplasms or brain metastasis or neurosurgical procedure OR multiple sclerosis or encephalitis or cerebrovascular disorder or intracranial hemorrhage or ischem* or apoplex* or insult* or stroke or nervous system malformation))*
  - Limitations: none
  - Sorting: Best match
  - Results: 377

  Included MeSH-Terms:

  central nervous system infections; tourette syndrome/pathology; intracranial hemorrhages; tics/etiology; head; central nervous system neoplasms; tourette syndrome/etiology; neoplasm metastasis; brain injuries; neurosurgical procedures; multiple sclerosis; gray matter; tics/pathology; tic disorders/pathology; wounds and injuries; leukoaraiosis; congenital abnormalities; cerebrovascular disorders; craniocerebral trauma; brain; encephalitis; nervous system malformations; tic disorders/etiology; tics; stroke

- Embase:
  - Date: 19.03.2020
  - Term: *(exp tic/et or exp tic/co or exp gilles de la tourette syndrome/et or exp gilles de la tourette syndrome/co or secondary tics.mp. or Tourettis*.mp.) AND ((exp brain damage/ or exp brain injury/ or exp head injury/ or posttraumatic.mp. or post-traumatic.mp. or (spinal injur* or spinal lesion*).mp. or exp white matter injury/ or exp white matter lesion/ or white matter abnormalit*.mp. or exp central nervous system infection/ or (gray matter lesion* or gray matter injur* or gray matter abnormalit*).mp. or exp brain malformation/ or exp wound/ or exp injury/ or exp central nervous system tumor/ or exp brain metastasis/ or exp neurosurgery/ or exp encephalitis/ or exp cerebrovascular accident/ or exp cerebrovascular disease/ or exp brain hemorrhage/ or (ischem* or stroke or apoplex*).mp. or exp nervous system malformation/))*
  - Limitations: none
  - Results: 205

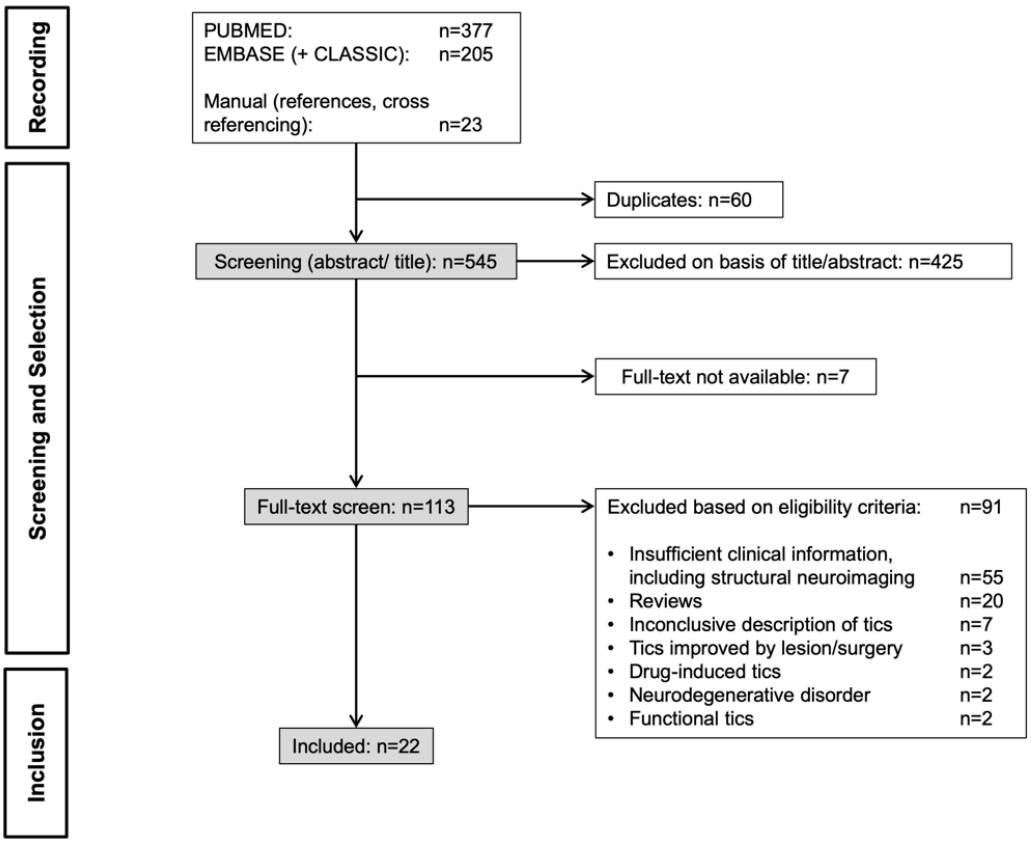

Supplementary Figure 1 Flow diagram of data acquisition.

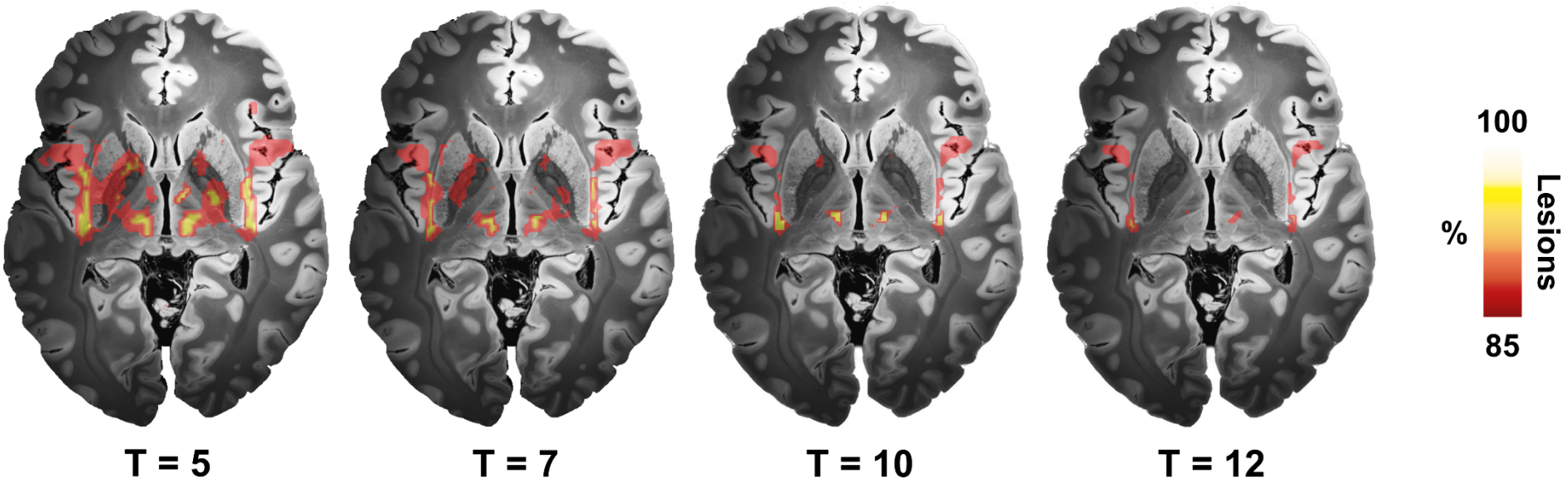

Supplementary Figure 2 Replication of lesion network map using different T-map thresholds. T indicates the T-score threshold used to generate different lesion network maps.

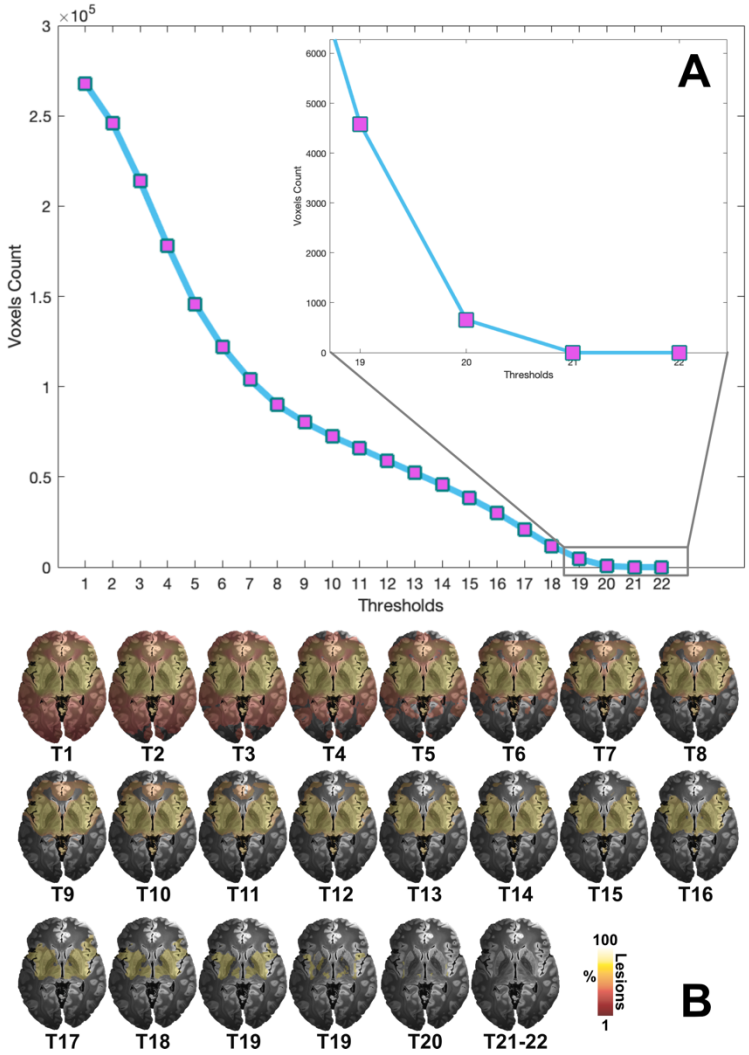

Supplementary Figure 3 (A) Lesion network map voxel count distribution in different thresholding levels indicated as number of lesions on the x axis. (**B**) Lesion network maps showing different distribution of voxels surviving the serial thresholding level (T).

Supplementary Table 1 Clinical characteristics of tic-inducing lesion cases

Case Nr/Ref	Year	Age at lesion confirmation (y)/Age at tic onset (y)/Sex	Latency to tic onset* (months)	Lesion etiology	Lesion captured [imaging modality]	Clinical tic characteristics	Suppressibility / Urges	Concurrent Movement Disorders[#]	Neuropsychiatric comorbidities	Sources of Funding
1[1]	2011	19/20/M	12	Traumatic brain injury	Scattered lesions in corpus callosum, right putamen capsule, dorsal aspect of mesencephalon and cerebral convexity (grey/white matter interface) [MRI]	Eyelid tics, facial grimacing, clenching fists; sniffing, grunting, throat clearing	Yes/Yes	Ataxia	Impulsivity, Attention and learning difficulties,	None reported
2[2]	2002	7/8/F	15	Traumatic brain injury	Lesion of the left putamen, globus pallidus, head of caudate, and internal capsule. [MRI]	Blinking, shoulder and arm jerks, trunk flexion, echopraxia; grunts, clicking noises, vocalisations, coprolalia, echolalia	Yes/NA	Ataxia	Short attention span, impaired short-term memory, disinhibited behavior	None reported
3[3]	2002	NA/8.5/M	6	Hemorrhagic stroke	Lesion of the right putamen and caudate nucleus [MRI]	Eye blinking, head jerking and shoulder shrugging, blowing air onto palm, compulsive scratching, head nodding, dystonic cervical tics, stretching and thrusting of neck; urge to sniff	Yes/Yes	Dystonia	ADHD, OCD, SIB (repetitive scratching)	NA
4[4]	2008	71/71/M	0.75	Ischemic stroke	Acute ischemic lesion of left caudate nucleus [MRI]	Vocalizations (“a”)	Yes/Yes	None	NA	NA
5[5]	2009	73/73/M	8	Ischemic lesions	Patchy ischemic lesions in the basal ganglia, periventricular white matter, centrum semiovale [MRI]	Nose picking, touching his nose, jerks on the legs, jumping up, blowing nose into handkerchief; shouting, startling	NA/Yes	None	Anxiety, Depression	NA
6[6]	2004	12/12/M	0.4	CO-Intoxication	Caudate nucleus and putamen bilaterally [MRI]	Repetitive smiling, speech arrest, shoulder shrugging, arm jerking, foot dorsiflexion, throat clearing, humming, lip smacking	NA/NA	None	NA	NA
7[7]	2003	4.5/4.7/M	2	VZV encephalitis	Changes of caudate nucleus head and putamen bilaterally, midbrain [MRI]	Head extension and flicking, upward eye deviation, nose twitching, shoulder shrugging; grunting, palilalia	NA/NA	Tremor	ADHD	Support from Action Research and the Barnwood House Trust

8[8]	1991	6/6/F	0.5	Herpes encephalitis	Extensive changes of right temporal lobe, basal ganglia and thalamus [CT, MRI]	Eye rolling, facial grimacing, head twitching, shoulder shrugging, jumping, touching objects and body parts, making obscene gestures; grunting, sniffing, snorting sounds	Yes/NA	Possibly dystonia (overflow movements)	Personality changes with emotional lability, anxiety and hyperactivity	Public Health Service Grant Support (NIH NS 27327; HD 25806)
9[9]	2020	28/35/M	84	Nail gunshot injury	Focal encephalomalacia of left parietal lobe [MRI]	Head turning; vocalisations ("me", "boo"), coprolalia	Yes/Yes	None	NA	None reported
10[10]	2012	52/52/M	10	Osmotic demyelination syndrome	Bilateral lesions of caudate nucleus and putamen, central pons and cortical areas, including insular and precentral cortex [MRI]	Dystonic tics of neck and shoulders; throat clearing	Yes/Yes	Parkinsonism	None	NA
11[11]	1997	33/26/M	NA	Traumatic brain injury@	Bilateral subcortical and periventricular leukoencephalopathic changes particularly of the frontal and the right temporoparietal white matter [MRI]	Nose rubbing, mouth opening, wringing hand movements, sniffing	No/No	None	Irritability, Distractibility, OCD, Depression	None reported
12[12]	2000	16/16/M	0.07	Arteriovenous malformation	Left frontal arteriovenous malformation [MRI]	Dystonic head turning, vocalisations ("yeah")	Yes/Yes	None	NA	NA
13[13]	1996	2/8/F	NA	Grade II astrocytoma^	Tumor involvement of optic chiasm, the hypothalamus and thalamus, internal capsule,ventral striatum, fornix, nucleus accumbens, septal nuclei, amygdala, and midbrain, including the substantia nigra and red nuclei [MRI]	Blinking, mouth-opening and other facial tics, throat clearing, lyrical vocal tic, adjusting glasses on nose until they felt "just right"	NA/NA	None	Aggression	Grant support (MH 49351; MH 18268; MH 30929; NIH RR 06022; HD 03008; 1K20MH01232-01; Tourette Syndrome Association)
14[14]	2009	30/30/F	NA	Multiple sclerosis	Lesions in white matter of both cerebral hemispheres, and the right cerebral peduncle, as well as the middle cerebellar peduncles and both thalami [MRI]	Blinking and other facial tics, throat clearing, palilalia, coprolalia	NA/Yes	Stereotypies	Restlessness, hyperactivity, mannerisms and stereotypies, poor impulse control, SIB	NA

									(repetitive scratching)	
15[15]	2016	NA/47/M	NA	Hypoxic brain injury	Bilateral pallidal lesions [MRI]	Blinking, forehead wrinkling and jaw deviation tics, as well as arm abduction, shoulder lifting and hip twisting tics	Yes/Yes	None	None	None reported
16[16]	2003	12/NA/M	NA	Hypoxic-ischaemic damage	Bilateral lesions of thalamic and infrathalamic structures. Involvement of right midbrain. High-signal lesion in left dorsolateral caudate-putamen, with involvement of internal capsule [MRI]	Blinking, grimacing and other facial tics, head jerks, body rocking, sounds and noises, including throat clearing, whistling, reiterative speech, as well as echo- and coprolalia	Yes/NA	Dystonia	Restricted social interaction, unusual preoccupations, fixed interests and rigid insistence. Inattentive, impulsive, violent outbursts. SIB (scratching, punching himself on abdomen and legs). Compulsive masturbation.	NA
17[17]	2002	34/34/F	NA	Multiple sclerosis	Lesions in the periventricular white matter, thalamus, basal ganglia and brainstem [MRI]	Throat clearing	Yes/No	None	Fatigue	NA
18[18]	1999	11/6/M	NA	Cystic malformations	Multiple cystic areas in the left gyrus rectus and superior frontal gyrus [MRI]	Eye and facial tics, vocalizations	NA/NA	None	No	NA
19[19]	2007	NA/NA/F	NA	Autoimmune encephalitis	Abnormal signal change in striatum bilaterally [MRI]	NA	NA/NA	Parkinsonism, Dystonia	OCB, Anxiety, Dysthymia	Tourette Syndrome Association; Sophie Cameron Trust; Action Research; NHS Trust; Marie Curie Training Fellowship)
20 [20]	2004	34/27/F	1	CO-Intoxication	Bilateral pallidal changes [MRI]	Facial tics with mouth opening, lateral jaw movements, neck twisting and shoulder shrugging.	Yes/Yes	None	NA	NA

21 [21]	1986	24/6/F	NA	Porencephalic cyst	Porencephalic cyst in right temporal love with involvement of basal ganglia structures [CT]	Tics of eyelids and mouth, and tongue protrusion tics. Head and shoulder tics. Diaphragmatic tics, coughs, grunting and vocalizations, including screams	NA/NA	None	NA	NA
22[22]	2016	16/16/M	NA	Acute necrotizing encephalopathy	Symmetrical T2-hyperintense lesions involving the basal ganglia (caudate, putamen and globus pallidus) and the thalami. Additional highly symmetrical white matter changes in the centrum semiovale [MRI]	Motor and vocal tics. Palilalia	NA/NA	Parkinsonism	ADHD, OCD, Tachygraphia	None reported

* from lesioning event to tic onset; # = including cerebellar signs; @ = Case 3 of the 3 reported. ^ = Case 1 of 3 reported. NA = Not Available, ADHD = Attention Deficit Hyperactivity Disorder, OCB/D = Obsessive Compulsive Behaviour/Disorder

Reference:

1. Ranjan N, Nair KP, Romanoski C, Singh R, Venketswara G. Tics after traumatic brain injury. Brain Inj. 2011;25:629-633.
2. Majumdar A, Appleton RE. Delayed and severe but transient Tourette syndrome after head injury. Pediatr Neurol. 2002;27:314-317.
3. Kwak CH, Jankovic J. Tourettism and dystonia after subcortical stroke. Mov Disord. 2002;17:821-825.
4. Gomis M, Puente V, Pont-Sunyer C, Oliveras C, Roquer J. Adult onset simple phonic tic after caudate stroke. Mov Disord. 2008;23:765-766.
5. Topçuoğlu V, Arman AR, Yazgan C, Arman A, Gönentür AG, Bicer DS. Tourettism in a 73 Year Old Man After Coronary Artery Bypass Surgery. 2009.
6. Alioglu Z, Boz C, Sari A, Aynaci M. Transient tic disorder following carbon monoxide poisoning. J Neuroradiol. 2004;31:231-233.
7. Dale RC, Church AJ, Heyman I. Striatal encephalitis after varicella zoster infection complicated by Tourettism. Mov Disord. 2003;18:1554-1556.
8. Northam RS, Singer HS. Postencephalitic acquired Tourette-like syndrome in a child. Neurology. 1991;41:592-593.
9. de Souza A. New-onset tic disorder following circumscribed brain injury. J Clin Neurosci. 2020;75:234-239.

10. Jung NY, Lee JH. Secondary tics after osmotic demyelination syndrome involving both the striatum and the cerebral cortex. J Clin Neurosci. 2012;19:179-180.

11. Krauss JK, Jankovic J. Tics secondary to craniocerebral trauma. Mov Disord. 1997;12:776-782.

12. Yochelson MR, David RG. New-onset tic disorder following acute hemorrhage of an arteriovenous malformation. J Child Neurol. 2000;15:769-771.

13. Peterson BS, Bronen RA, Duncan CC. Three cases of symptom change in Tourette's syndrome and obsessive-compulsive disorder associated with paediatric cerebral malignancies. J Neurol Neurosurg Psychiatry. 1996;61:497-505.

14. Nociti V, Fasano A, Bentivoglio AR, et al. Tourettism in multiple sclerosis: a case report. J Neurol Sci. 2009;287:288-290.

15. Criscuolo C, D'Amico A, Peluso S, Popolizio T, Pellecchia MT. Adult-onset pure tic disorder after post-traumatic hypoxic lesions of the globus pallidus. Parkinsonism & related disorders. 2017;34:75-76.

16. Berthier ML, Kulisevsky J, Asenjo B, Aparicio J, Lara D. Comorbid Asperger and Tourette syndromes with localized mesencephalic, infrathalamic, thalamic, and striatal damage. Dev Med Child Neurol. 2003;45:207-212.

17. Lana-Peixoto MA, Teixeira AL, Brazilian Committee for T, Research in Multiple S. Simple phonic tic in multiple sclerosis. Mult Scler. 2002;8:510-511.

18. McAbee GN, Wark JE, Manning A. Tourette syndrome associated with unilateral cystic changes in the gyrus rectus. Pediatr Neurol. 1999;20:322-324.

19. Martino D, Church A, Giovannoni G. Are antibasal ganglia antibodies important, and clinically useful? Pract Neurol. 2007;7:32-41.

20. Ko SB, Ahn TB, Kim JM, Kim Y, Jeon BS. A case of adult onset tic disorder following carbon monoxide intoxication. Can J Neurol Sci. 2004;31:268-270.

21. Kjaer M, Boris P, Hansen LG. Abnormal CT scan in a patient with Gilles de la Tourette syndrome. Neuroradiology. 1986;28:362-363.

22. Boca M, Lloyd K, Likeman M, Jardine P, Whone A. Basal ganglia necrosis: a 'best-fit' approach. Pract Neurol. 2016;16:458-461.